Green Chemistry

ROYAL SOCIETY OF CHEMISTRY

CRITICAL REVIEW

View Article Online
View Journal | View Issue

Cite this: *Green Chem.*, 2024, **26**, 10718

Monoliths enabling biocatalysis in flow chemistry

Aleksandra Lambarska,[a,b] Katarzyna Szymańska *[a] and Ulf Hanefeld *[b]

Received 18th July 2024,
Accepted 25th September 2024

DOI: 10.1039/d4gc03535f

rsc.li/greenchem

This is a review on the feasibility of monolithic porous supports in biocatalysis carried out in a continuous flow system. It discusses factors affecting the efficiency and stability of enzyme immobilisation, kinetic parameters of enzyme processes carried out inside a monolith, biocatalysis in single and two-phase systems, and cascade reactions including cofactor regeneration. It also covers materials engineering (monolith types) and issues related to the flow of reactants through the monolith (chemical engineering). Emphasis is placed on the fact that the application of (bio)catalysis improves selectivity and atom economy, thus lowering the *E* factor. However, biocatalysts need to be employed in a reactor, which can aid further improvement towards green chemistry goals. The application of enzymes in flow chemistry has been shown to lead to higher space time yields (STYs) compared to batch reactions. In particular, with monolithic reactors a drastic decrease in volume and thus solvent can be achieved. By immobilising very high densities of enzymes directly on the monolith, reaction times dwindle, improving STYs. The small reaction volumes enable excellent heat transfer, helping to save energy. The underlying principles of monolithic flow reactors and their application in mono- and bi-phasic biocatalytic systems will be examined.

1. Introduction

Enzymes provide excellent selectivity in chemical reactions. The industrial application of biocatalysis has therefore increased and it enables processes from bulk to fine chemicals and pharmaceuticals.[1–4] These new enzyme-based approaches reduce the number of synthesis steps and decrease the demand for stoichiometric amounts of chemicals while also shortening the time of synthesis,[2–4] with the synthesis of molnupiravir being a perfect example of this (Scheme 1).[5] Due to this fact, the processes using enzymes as catalysts are often referred to as "white biotechnology", underlining their positive impact on the environment.[1] With this increase in demand, new technologies for the application of enzymes need to be developed.[1] In addition to the classical fed-batch reactor many new approaches, such as parallel reactors and flow chemistry, have entered the market for experimental purposes.[6–11]

The industrial use of enzymes on a truly large, multi-ton scale, in particular in a continuous process, requires their immobilisation on a suitable support, enabling the use of a dedicated reactor system.[7,12] Most of the carriers used in immobilisation are powders, or more coarsely granulated products, typically applied in batch reactors with intensive mechanical stirring. However, their drawback is gradual size reduction during the process, which negatively affects their properties and hinders their separation. Moreover, due to the necessity to ensure intensive mass transfer in the suspended matter, the amount of the heterogeneous catalyst is limited, which directly affects the efficiency of the process. Additionally, in batch applications, scaling up causes problems related to heat and mass transfer and mixing. Ideally, initial laboratory experiments with immobilised enzymes that ensure recycling could be straightforwardly transferred to industrial settings.

Low-volume flow reactors (microreactors) are a solution that allows amelioration of some of these difficulties.[13–17] The problems related to scaling up in the case of using microreactors are resolved by numbering up a single reactor. This eliminates the necessity to design and build a pilot system. However, it does require the correct design of the reactor setup in a parallel or sequential system. In the applied microreactors, the diameters of the channels are usually 0.1–0.5 mm. Such small channel diameters force the use of a laminar flow regime and therefore the mixing (diffusion) time of molecules (t) is proportional to the square of the channel width/diameter (L):

$$t \sim \frac{L^2}{D}$$

where D is the diffusion coefficient of a molecule. When L is reduced to 1/10, the diffusion time is reduced to 1/100 and the fluid can be mixed 100 times faster.[13] Shortening the mixing

[a]*Department of Chemical Engineering and Process Design, Silesian University of Technology, Ks. M. Strzody 7, 44-100 Gliwice, Poland. E-mail: Katarzyna.Szymanska@polsl.pl*
[b]*Biokatalyse, Afdeling Biotechnologie, Technische Universiteit Delft, Van der Maasweg 9, 2629 HZ Delft, The Netherlands. E-mail: U.Hanefeld@tudelft.nl*

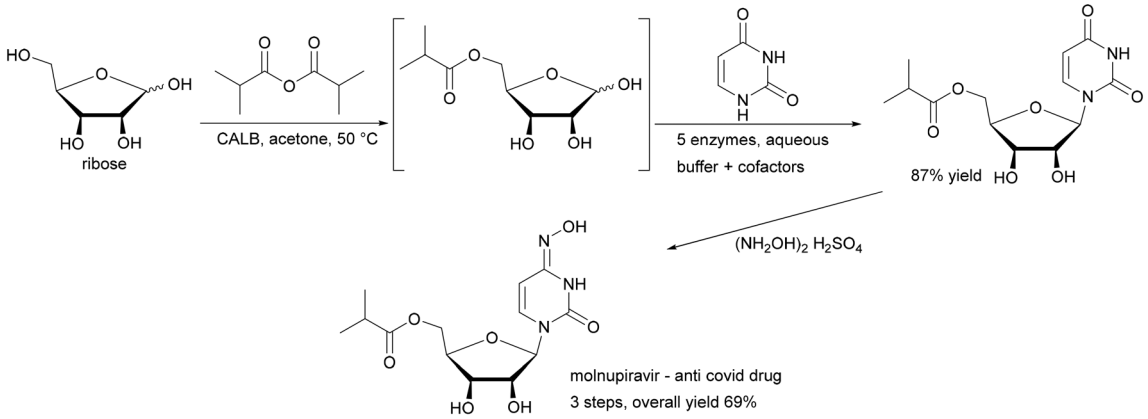

Scheme 1 Enzymatic strategy for obtaining molnupiravir in just 3 steps.

time intensifies the transfer of heat and mass. Due to the small volume of the reactor and the sizes of the channels, the ratio of the active surface of the reactor to the volume of the reaction mixture is significantly increased, which results in the increase of volumetric productivity and the decrease of investment costs. In addition, the intensification of mass and heat transfer and the increase in the surface area to volume ratio significantly increase process rates. Increased process rates in turn reduce process time and energy consumption, lowering operating costs and benefiting the environment. The small reaction volume not only favours the reduction of the exploitation risk, especially in the case of exothermic reactions or reactions with hazardous substances, but also reduces the amount of post-processing waste. Additionally, the enzyme is immobilised and not even a filtration step is necessary.[13–15,18–20]

The microreactors (Fig. 1) that attract the most attention are:

• "lab-on-the-chip" type microreactors – usually they are either a single platelet or a stack thereof, with a network of channels with micrometric diameters. These reactors are usually intended for homogeneous reactions and applied in chemical and medical analytics.[21,22] The key disadvantage is that no immobilised enzymes can be applied, ruling them out for large-scale applications.

• capillary microreactors – they are a single capillary or a bunch thereof, usually with a very thin catalytic film placed on the internal surface of the walls.[23] Here enzymes can be immobilised. The disadvantage is however the straight shape of the channel. This does not intensify the mixing due to laminar flow and therefore the mass and heat exchange can be modest.

From left to right: Katarzyna Szymańska, Aleksandra Lambarska and Ulf Hanefeld.

Katarzyna Szymańska received her Ph.D. in 2009 from the Faculty of Chemistry, Silesian University of Technology, Gliwice, Poland. Her research interests include engineering of (bio)heterogeneous catalysts, nanostructured materials, and chemical and enzymatic microreactors. She is currently a professor at the Department of Chemical Engineering and Process Design, SUT, Gliwice, Poland, and collaborates with Prof. U. Hanefeld, Prof. P.L. Hagedoorn (TU Delft), E. Magner (University of Limerick), Prof. D. Tischler (RUB), and P. Walde (ETH).

Aleksandra Lambarska received her M.Sc. and B.Sc. degrees in biotechnology from the Silesian University of Technology (Poland) in 2022 and 2021 under the supervision of Assoc. Prof. Katarzyna Szymańska. She is currently a Ph.D. student at the same university. She started her Ph.D. journey with an internship at Technische Universiteit Delft (the Netherlands) under the supervision of Prof. Ulf Hanefeld. Her research interests focus on heterogeneous biocatalysis, enzyme immobilisation and their application in continuous flow processes.

Ulf Hanefeld received his PhD from the Georg-August-Universität zu Göttingen, having performed the research both with Prof. H. Laatsch (Göttingen) and Prof. H. G. Floss (Seattle). After postdoctoral years with Prof. C. W. Rees (Imperial College London), Prof. J. Staunton (Cambridge) and Prof. J. J. Heijnen and Dr A. J. J. Straathof (TU Delft), he stayed at the Technische Universiteit Delft and his research in Delft focuses on enzymes and their immobilisation and application in organic synthesis.

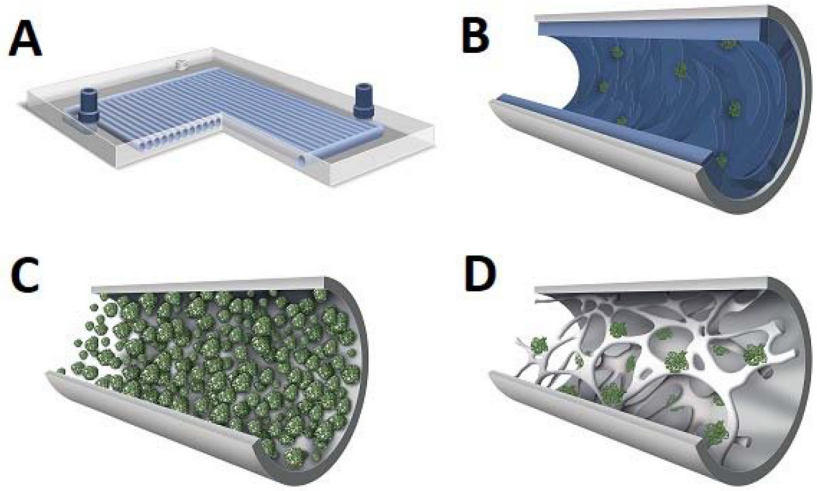

Fig. 1 Types of microreactors: lab-on-the-chip (A), capillary (B), packed-bed (C), and structural/monolithic (D).

• packed bed microreactors – in these reactors, the fine-grained bed of the catalyst fills the capillary/tube and the reactants flow in the annular space between the catalyst grains. These reactors are easy to build but the drawback is the relatively high flow resistance, which can further increase as a result of bed compression.[24]

• structural microreactors or monoliths – the core of the reactor is constituted by a porous structure/monolith with open pores/channels connected with each other – the catalyst is then immobilised either on the surface of the monolith structure or (optimally) in its pores if it exhibits a two/three-modal porous structure, and reactants flow through the meandering pores.[25,26] The continuous monolith structure ensures flow stability and virtually eliminates bed compression (especially with inorganic monoliths).

Overall the monolithic reactors combine all the advantages of continuous flow microreactors. At the same time they do not suffer from back pressure problems and bed compression and create turbulence during flow for ideal mixing, and enzymes can be immobilised on the reactor walls. We have recently summarized our own contribution to that field.[27]

Microreactor technology is mainly applicable to low-scale processes where large quantities of the final product are not required. The small geometric size of the microreactors makes it possible to create a suitable installation in a short time and in virtually any location, reducing the carbon footprint associated with transport. Adamo *et al.*[28] have recently described a demonstration system that can carry out continuous synthesis and formulation of active pharmaceutical ingredients (APIs) in a refrigerator-sized unit.

In this review the kinetic argument for the advantages of flow chemistry and in particular the application of monolithic microreactors and their application in continuous-flow biosynthesis (Fig. 2) is made. This leads to the possibility of using small reaction volumes and better surface area to volume ratios, which reduces energy consumption.

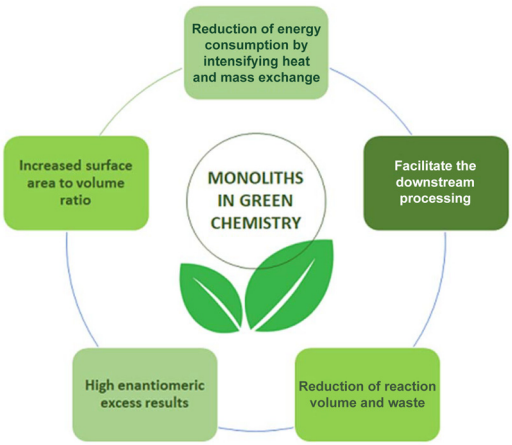

Fig. 2 Development of biocatalysis and microreactor technology in the field of green chemistry.

At the same time, better reaction control leads to higher selectivity, thus less waste and straightforward downstream processing (DSP). Improved DSP and higher STY values both contribute to achieving lower environmental (*E*) factor values. For both single reactions and reaction cascades, in single-phase or biphasic systems and under consideration of cofactors, this will be discussed and the advantages of monolithic microreactors will be demonstrated. In particular the perspective of green chemistry will be considered. The *E* factor as well as Green Chemistry Principles will be critically applied.

2. Monoliths

2.1 Types of monoliths

The word monolith comes from the Greek word 'mono lithos', meaning a single stone. In materials engineering it means a

material in 'one piece'. The automotive industry was one of the first industries to use monoliths. They are produced by extrusion and the most common material obtained is cordierite, which is used as a carrier for catalytic converters in the exhaust of cars.[29,30] Monoliths are also made from metals, mullite (a mixture of silicon and aluminum oxides in a 2 : 3 ratio) and silicon carbides. Their disadvantage is a small specific surface area (0.7 m^2 g^{-1} for cordierite) and they are therefore less widely used in other industries.[30] Modern monolithic supports overcome these problems. Generally, monolithic carriers are divided into organic/polymer and inorganic (mostly silica and carbon) groups.[31–38] The former are characterized by good biocompatibility, pH stability and the presence of various functional groups; however, their limited resistance to organic solvents may lead to changes in the porous structure and thus decrease their mechanical stability.[39] Inorganic structures on the other hand are very stable and these kinds of monoliths additionally offer very good permeability, both for organic and inorganic solvents.[34–37] Oxide-based inorganic monoliths (*e.g.* silicon, aluminum and titanium oxides) can be obtained in several ways. Firstly, there are methods using templates such as colloidal particles (*e.g.* latex or polystyrene beads), ionic liquids, starch, cellulose and many others.[40–44] The process involves introducing an inorganic precursor solution into the free spaces created by packing the template. In the next step, the system undergoes condensation and crystallization followed by the removal of the template, usually by calcination or extraction. This leads to the formation of ordered macro/mesoporous materials in which both types of pores are through-going and interpenetrating.

A macro/mesoporous structure can also be created by chemical reaction-induced phase separation. This phenomenon was first used by Nakanishi *et al.*[45–49] and the method was later modified by, among others, Smått.[50] A polymer (*e.g.* polyethylene oxide) is used to induce phase separation. Phase separation results in the formation of a solvent-rich phase and a polymer-rich phase. The polymer phase solidifies by gelation of the silica precursors within it, forming a micrometric skeleton, while the solvent-rich phase forms macropores after evaporation. The ratio of reactants and the process conditions allow the control of the structural parameters, *i.e.* the macro/mesopore sizes, the specific surface area and the total volume of the pores, covering a wide range.[26,36–38] Oxide-based inorganic monoliths can be used in catalysis[51–57] as liquid chromatography columns[58,59] or controlled drug release systems.[60,61]

The most common route to synthesize self-supported carbon monoliths with multilevel porous structures relies on the carbonization of porous polymers[62–66] and biomass.[67–69] Another route makes use of an inorganic porous material with a uniform channel system as a hard template. The template is filled with carbon precursors which are internally carbonized and then the inorganic template is removed.[70–72] Carbon monoliths have been used as supercapacitors,[62,69] microextraction fibers,[66] microreactors,[63,73] electrochemical sensors,[67,68,70] and sorbents.[74]

Organic polymer monoliths have been considered good supports for enzyme immobilisation owing to their good biocompatibility, excellent pH stability and ease of modification with various functional groups.[75–79] The known procedures for making polymer monoliths are simple 'one-pot' synthesis, where the monomers, initiators, cross-linkers and pyrogenic solvents are simply pre-mixed before being filled into a capillary and then exposed to factors such as UV light or heat to initiate polymerization.[31,80,81] Polymer monoliths are widely used primarily in different kinds of chromatography methods,[82,83] solid-phase extraction,[84,85] for the preparation of flow-through immobilised enzyme reactors (IMERs) suitable for proteomics,[86–90] microfluidic analysis,[91,92] pharmaceutics,[93,94] biodiesel[95] and oligosaccharide[96,97] production, *etc.*

Monoliths can also be produced using additive manufacturing, commonly referred to as 3D printing, which is an emerging bottom-up manufacturing technology with the potential to achieve rapid prototyping of complex geometries and structures, even with sophisticated internal structures (pores or complex channels).[98,99] A wide range of materials can be utilized in 3D fabrication, which can be classified into three main categories: polymers, ceramics, and metals.[100] Furthermore, the chemical modification of printed materials is also attracting increasing attention: by modifying the printed carriers, enzymes can be immobilised on them.[101–106]

2.2 Flow behaviour in monoliths

While considering the potential of microreactors for continuous processes, one should note that the flow in small-diameter straight channels is laminar in the entire range of the applied conditions. For that reason, mixing and transportation to catalytic centres located on the surface is slow compared to the mixing observed in turbulent flow.[107,108] Mixing is diffusion limited in the absence of turbulent flow. Although it is possible to elongate the channel system to allow diffusion to complete as the fluid is transported through the microsystem, it also requires a longer channel and thus reaction time. Several strategies have been devised to speed up mixing processes actively in microfluidic systems. Bessoth *et al.*[109] proposed to split a liquid flow into even smaller channels, where the diffusion distances become so small that the corresponding mixing times by diffusion were in the order of milliseconds. Later, all divided streams were combined again downstream.[109] To intensify the mixing, the introduction of baffles was proposed[110] as well as using ultrasound[111] or introducing fragments of porous structures.[112,113] For these reasons, monoliths characterized by a very high number of interconnected tortuous channels and micrometric diameters seem to be an interesting solution. The tortuous character of the channels causes sudden changes in the direction of the flow of the liquid, which fosters the formation of swirls, the intensification of mixing and the contact between the liquid and the wall of the microchannel (Fig. 3). Their small diameter additionally intensifies the exchange of mass and heat. However, this could increase the back pressure. The flow of liquid through monolith structures is complex from a microscale perspective and

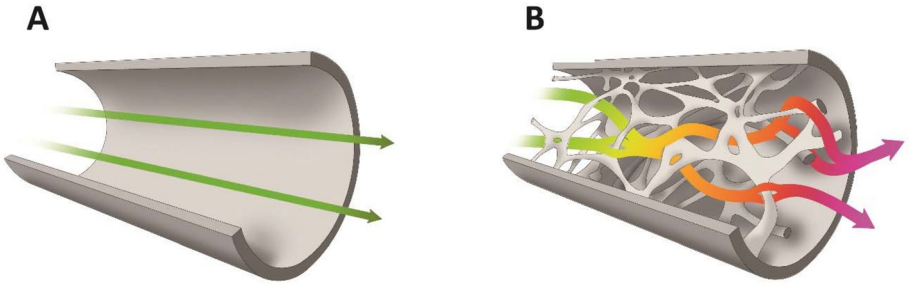

Fig. 3 Scheme of liquid flow in a straight channel (A) and in structured monoliths (B).

tends to obey Darcy's law.[26,114] The relationships between the pressure drop gradient ($\Delta P/L$) and the volumetric flow rate of liquid ($\dot{V}$), its viscosity (η) and the cross-sectional area of the monolith (A) are given by the Darcy–Weisbach equation:

$$\frac{\Delta P}{L} = \frac{1}{K}\frac{\eta}{A}\dot{V}$$

where the permeability coefficient (K) is proportional to the diameter of the macropores ($K \sim d^2$). As was shown by Szymańska *et al.*[26] the monoliths with macropore diameters in the range 20–40 μm allowed for applying flow ranges of 200–700 cm^3 $(cm^{2-}$ $min)^{-1}$ at pressure gradients falling in the range of 15–65 kPa cm^{-1}. A decrease of macropore diameter to 10–12 μm caused comparable decreases in pressure, however, at much smaller flow rates (50–200 cm^3 $(cm^{2-}$ $min)^{-1}$). A low pressure decrease allows for simple and thus cost-efficient metering pumps while permitting them to operate at increased linear speeds of flow (intensification of the mass transport) and at flow rates of reacting substances measured in tens and hundreds of cm^3 min^{-1}. This opens the possibility of multi-kilogram syntheses in cm^3 reactors. These amounts are in stark contrast with the values characterizing typical microfluidic reactors, where the applied flow rates are limited to tens and hundreds of μm^3 min^{-1}.[86,115]

In processes where the reactants are in two phases (biphasic processes), mass transfer in microchannels becomes even more important and depends on the flow patterns. A common pattern is segmented or plug flow, where one phase forms drops, the sizes of which are as large as the channel diameter (plugs) separating the continuous phase into segments (slugs) (Fig. 4A).[116] The overall mass transfer rates depend on the plug geometry. In addition, the wall wetting properties might result in the formation of a thin film between the plugs and the wall, which increases the specific interfacial area available for mass transfer. The latter is also intensified through internal circulation within the slugs or the plugs caused by the shear between the continuous phase/wall surface and the slug or plug axis, which enhances diffusive penetration.[117–121] In certain situations, especially in straight channels, the advantage provided by the increased interfacial area and mixing effects may be insufficient to balance the short residence time. Many methods for increasing the mixing effects in a straight channel microreactor were developed such as ultrasound[122–125] and magnetic nanoparticle addition.[126–129] A straightforward and elegant strategy was demonstrated by Abraham *et al.*,[130] who changed the dimension of the circular microchannel (*via* a sudden expansion and then a sudden contraction), increasing the slug and droplet diameter and reducing the length (and *vice versa*). This type of transformation alters the concentration field and positively interferes with the internal mixing in the slugs and droplets. As the shear stress plays an important role in triggering the internal circulations inside the fluid elements, the flow through a non-uniform channel improves the extraction efficiency. A similar effect will be obtained using the structural/monolithic microreactors.[26,131–133] The use of monolithic microreactors ensures a favourable surface-to-volume ratio and the presence of meandering channels further improves mixing and thereby increases the transport of mass

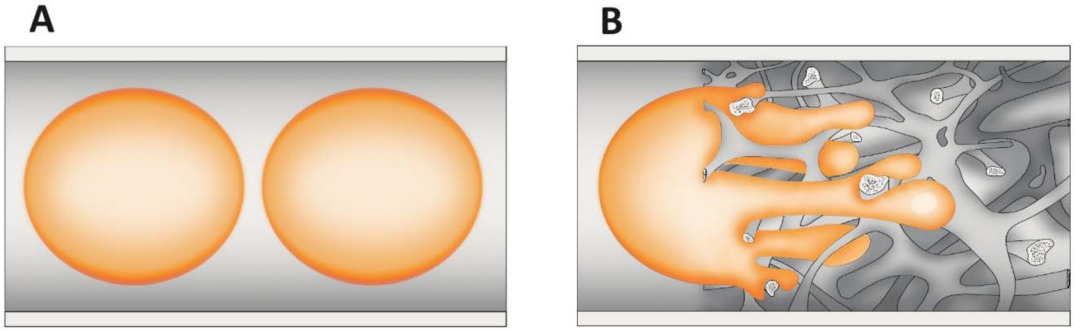

Fig. 4 Scheme of biphasic flow in a straight channel (A) and in structured monoliths (B).

and heat between phases (Fig. 4B). The meandering structure of the silica monolith will induce changes in the flow of a single droplet and thus not only enhance the interface between the continuous and dispersed phases but also intensify the internal circulation within the slugs or the plugs, which in turn has a positive effect on mass transport.

3. Biocatalysis in monoliths

3.1 Attaching the enzyme to the monolith

The application of catalysts in general and specifically enzymes always requires their removal at the end of the reaction. Immobilisation of the enzymes greatly eases this downstream processing (DSP) and at the same time often improves the stability of the biocatalysts. This is achieved by single or multi-point interaction with the carrier's surface and it generates a favourable micro-environment and protection against intermolecular interactions.[134–137] As an additional advantage it enables reuse and reduction of process costs.[134,138] The application of immobilised enzymes furthermore allows for a significant simplification of the reactor's structure and for controlling the process, *e.g.* stopping it by separating the catalyst from the reaction mixture. Due to the above, the immobilisation of enzymes is often performed in large-scale industrial applications.[136,137] The first reports on immobilised enzymes date back to 1916,[139] while their commercial use first took place in the 1960s.[140] Today immobilised Penicillin G acylase is reused[141] up to 1000 times and immobilised glucose isomerase[7,142] is at the core of the high fructose corn syrup process.

There is no universal immobilisation technique to acquire an active and stable preparation. While designing the immobilisation method, many factors must be considered, including:[134,136,143]

- interactions: enzyme–substrate/product, enzyme–carrier, substrate/product–carrier;
- resistance of the carrier to reaction conditions (solvent, temperature, pH, *etc.*);
- the reactor type used: tank reactor with mixing, membrane reactor, microreactor.

However, the most important factor influencing the effective attachment of enzymes is the presence of appropriate functional groups on the carrier surface. Functional groups must provide a suitable microenvironment for the expression of enzyme activity and ensure the stability of the biocatalyst.

By immobilising enzymes on the surface/inside the pore of a monolith, it is possible to use all known techniques for binding the enzyme to a solid support (covalent binding, physical and ionic adsorption, transition metal complexation). These techniques have already been described in detail in numerous reviews[137,144–146] and will therefore not be discussed here. Due to the number of factors affecting the immobilisation process, it is very difficult to determine *a priori* which of the mentioned techniques is superior. The dominant opinion is that it is necessary to determine the parameters individually for each selected enzyme, especially considering that the forces acting on the immobilised enzyme in a flow system are significantly different from those in a batch reactor.[15,69–74]

Enzyme immobilisation is critical when considering continuous processes. To highlight its importance, a few representative examples are given. One of the most important performance parameters of flow microreactors is their process stability. The use of different methods of enzyme immobilisation results in different strengths of enzyme–carrier interactions. The continuous flow of reactants through the monolith can favour leaching of the enzyme from its surface. In a study by van den Biggelaar *et al.*,[147] transaminases were immobilised on macrocellular silica monoliths functionalised with amino groups. Two immobilisation techniques were used: adsorption *via* ionic interactions and a covalent method using an amino-functionalised monolith and glutaraldehyde as a coupling agent, but only the latter method gave stable bioreactors. Decreases in activity were explained by the leaching of the enzyme from the support. Similar results were obtained in the work of Szymańska *et al.*[26] where trypsin was adsorbed on cyano-functionalised silica and covalently immobilised on amino-functionalised silica using glutaraldehyde as a linker. The adsorbed trypsin showed a higher initial activity, but there was a significant decrease in the activity over time. In the case of covalent binding, the enzyme retained its initial activity. As in previous work, the observed effects (decrease in activity) were explained by the leaching of the adsorbed enzyme from the support surface. Adsorption was also used for the deposition of lipase on a hydrophobised silica monolith,[133] and the obtained catalyst/reactor was used in the kinetic resolution of the non-equimolar mixture ($S:R = 85:15$) of the secondary allylic alcohol (+)-1-[(1*S*,5*R*)-6,6-dimethylbicyclo[3.1.0]hex-2-en-2-yl]ethanol. Interestingly, the adsorption method used in this case allowed the reactor to operate stably for about 120 h. The main difference between the cases described is that in the first two processes, the reactions were carried out using an aqueous solvent, whereas the kinetic resolution was carried out in an organic solvent. Enzymes have a high affinity for water, so the use of this solvent favours the leaching of the enzyme from the support. By using an organic solvent, the leaching can be drastically reduced.

This was also noted for hydroxynitrile lyases (HNLs). When applied for cyanohydrin synthesis, the reactions were performed in buffer saturated organic solvents and no enzyme leaching was observed.[148–151] In contrast when the non-natural Henry reaction was catalysed, water was necessary and leaching occurred.[152] The strength of the enzyme–carrier interaction is not the only factor affecting stable reactor performance. A critical issue may be the immobilisation method itself. In the work of Shortall *et al.*[153] lactate dehydrogenase (LDH) was immobilised *via* two different methods: electrochemical entrapment in poly(3,4-ethylenedioxypyrrole) and covalent attachment on glyoxyl agarose. Both reactors allowed for up to 100% conversion of NADH; however, LDH@agarose proved superior in terms of reuse and storage. In this case, no leach-

ing of the enzyme was observed and the loss of activity was explained by the stability of the enzyme itself.

The covalent bond between the enzyme and the support can be direct, *i.e.* the functional groups of the support bind covalently to the side group of the amino acid, or indirect through the introduction of a linker (*e.g.* glutaraldehyde). In principle, this does not affect the leaching of the enzyme, but it can affect the activity and stability of the enzyme. Yao *et al.*[31] compared two methods for the covalent immobilisation of trypsin on polymer monoliths. The first, termed 'one-step', involved the direct formation of a covalent bond between the epoxy group of the support and the enzyme. The second, termed 'multi-step', involved the modification of the epoxide group with a diamine followed by activation with glutaraldehyde. The researchers showed that the 'multi-step' method produced catalysts/reactors with higher activity. Similar studies can be found in ref. 154 where ribonuclease A was immobilised by the direct reaction between the amino groups of the enzyme and the epoxy groups of the sorbent and the reaction of the enzyme with the aldehyde-containing polymer spacer preliminarily bound to the surface of the monolith. In this case, the introduction of the linker did not result in any change in enzyme activity. This shows that the introduction of the linker, and therefore the distance of the enzyme from the surface of the monolith, does not have a unidirectional effect on the activity of the enzyme and that each case must be considered individually.

Another important parameter affecting the immobilisation of enzymes within the monolith structure is the uniform distribution of functional groups. This is particularly important when functional groups are introduced after the monolith preparation/synthesis step. The work of van den Biggelaar *et al.*[155] compared methods for introducing an amino group onto the surface of a silica monolith and found that the essential parameters that allow reaching high catalytic performance were the functionalisation mode (dry *versus* wet) and water availability during the functionalisation process. In practice, briefly dipping the monolith in the functionalisation solution followed by aging under a solvent-saturated atmosphere allowed obtaining a homogeneous functional group dispersion throughout the entire monolith. Total water control during the process (by using dried monoliths and water-saturated solvent) allowed minimizing the batch-to-batch variability which affects enzyme immobilisation and biocatalyst efficiency. Equally important, the immobilisation of biocatalysts will enable the reuse of enzymes and support the DSP process.

3.2 Microbial infection in the monolith

Optimal aqueous reaction conditions for most enzymes (neutral pH values, room temperature) are also optimal conditions for the growth of various microorganisms. The risk increases even more when the substrates are an easy source of carbon or nitrogen as a growth medium. Moreover, there is a whole range of microorganisms, primarily fungi, that are able to not only survive but also thrive under slightly more extreme conditions, such as high temperature (above 40 °C) and low pH values (below pH 5). A solution of standard antibiotics such as penicillin can be utilised to eliminate the microbiological infection while preserving the initial catalytic activity of the immobilised enzyme protein. However, carrying out such a procedure only allows curing the symptoms but not elimination of the cause. Therefore, microbial contamination inside monolithic industrial microreactors can be a serious problem due to difficulties in dismantling for cleaning purposes. To overcome this obstacle, a practical solution is to filter all solutions before use and to maintain sterile conditions throughout the process to prevent bacterial/fungal infections. Also low concentrations of microbial growth inhibitors, such as for example sodium azide (NaN_3),[156,157] can be employed. However, the most important factor is the hygiene of the process.

Interestingly, monolithic microreactors can be used to detect bacteria in biological samples. One solution is to use an immunoreactive filter in a microporous polyacrylamide monolith. Due to size exclusion, bacteria interact with the surface of the filter and become stained. This solution can provide an alternative for infection diagnosis.[158,159]

3.3 Kinetics in monoliths

As established by Michaelis and Menten, the rate of an enzymatic reaction depends on the substrate concentration. The initial increase in the rate is linear and proportional to the increase in substrate concentration. The maximum reaction rate (V_{max}) is reached when the enzyme is completely saturated with the substrate. Further increases in substrate concentration will not increase the reaction rate. For enzymes, this typically occurs at lower substrate concentrations than for other catalysts. The reaction rate can be increased by the amount of enzyme available, provided of course that the amount of substrate is significantly higher than the amount of enzyme. The above considerations apply to enzymatic reactions catalysed by a non-immobilised enzyme.

The case is slightly different when an immobilised enzyme is considered. In general the increase of the amount of enzyme on the support is desirable to enhance the enzyme/substrate ratio and thus the reaction rate. On the other hand, the kinetics of the reaction is significantly influenced by the accessibility of the active site of the immobilised enzyme. Consequently, the effect of enzyme density on the surface of the solid support must be considered as a critical parameter affecting the availability of the active site of the enzyme.[157] This means that diffusion is also now a key parameter.

To study the influence of substrate size on diffusion, Volokitina *et al.*[160] immobilised ribonuclease A on polymeric monoliths for the hydrolysis of a small and a large substrate (cytidine-2′,3′-cyclic monophosphate monosodium salt (CCP) and RNA). Columns with pore sizes of 450, 830, 1220 and 2020 nm were prepared and the enzyme was embedded in them. Both the small molecule substrate (CCP) and the large molecule substrate (RNA) were hydrolysed. As expected for the small-molecule substrate, they showed that both the molecular recognition process (convergence of K_M values) and the bioca-

talytic activity did not depend on the average pore size of the monolithic stationary phase. The results obtained indirectly prove that the mass transfer mechanism is the same in all the columns tested and, consequently, that the process of enzyme–substrate complex formation takes place in the same way.

Completely different results were obtained for the macromolecular substrate.[160] In this case, a clear effect of pore size on RNA hydrolysis was observed, as it was found that the degree of substrate hydrolysis increased with increasing pore size. With macromolecular substrates, the enzyme must sequentially hydrolyse all possible bonds in the macromolecule to convert it into a series of resulting products. Unlike the reaction in solution, this situation may be complicated for immobilised enzymes due to steric limitations. They reduce the accessibility of the enzyme's active site for the large substrate molecule. Furthermore, the use of macromolecular substrates leads to a reduction in mass transfer, *i.e.* a reduction in the contact time between the enzyme and the substrate, which in turn can lead to a reduction in reactor efficiency. In this regard, pore characteristics[161] can play a significant role in the degradation of high molecular weight substrates.[160]

Another parameter that influences the kinetics of the reaction taking place inside the monolith is the chemical nature of the monolith surface and, related to this, the way in which the enzyme is immobilised. Luangon *et al.*[63] adsorbed *Candida rugosa* lipase on a hierarchical porous carbon monolith with micropores on an interconnected macroporous skeleton synthesized through the sol–gel polycondensation of resorcinol and formaldehyde. The effects of the oxygenated surface of micro-/macroporous carbon monoliths on lipase immobilisation were investigated. The estimated values of V_{max} and K_M of immobilised lipase on a crude carbon monolithic column are approximately 2 times lower than the values of V_{max} and K_M obtained from an oxygenated carbon monolithic column. Although the protein binding efficiencies of crude and oxygenated columns are similar, the carbon monolith with the oxygenated surface exhibits clearly higher efficiency compared with the untreated surface carbon monolith. Thus, the oxygenated surface of the micro-/macroporous carbon monolith exhibits a better transesterification rate. An improvement in the transesterification rate can be explained by an induction of a slightly polar substrate *p*-nitrophenyl palmitate (*p*-NPP) by the oxygenated surface of the micro-/macroporous carbon monolith or by better stabilization of lipase by the oxygenated carbon surface.

The influence of the chemical nature of the monolith surface and the associated immobilisation method is of importance[162] but not relevant in all cases. The work described by Volokitina *et al.*[154] compared two methods of immobilising ribonuclease A (RNase A) on a methacrylate-based polymer monolith. In the first case, the biocatalyst molecule was attached to the solid surface by direct covalent bonding, while in the second case, a flexible-chain synthetic polymer was used as an intermediate spacer. The values of K_M determined for the hydrolysis of polynucleotide by bound RNase were 0.76 mM for direct immobilisation and 0.56 mM for immobilisation with a polymer spacer. The similar K_M values confirm their practically identical enzyme–substrate binding strength. The specific activity values were found to be quite similar for both immobilisation methods, demonstrating the maximum activity of the biocatalyst bound in different ways.

From the point of view of flow processes, it is also interesting to compare the kinetic parameters of enzymes immobilised inside the monolith with those immobilised on silica powder and applied in a batch system. Does flow efficiently suppress diffusion limitations caused by immobilisation? When immobilising invertase in a silica monolith,[56] the K_M value was similar for those immobilised on particles, but the V_{max} value was approximately 1500 times higher for invertase immobilised in the monolith. While at first glance unlikely, it is justified by the amount of enzyme present in the reaction zone. For the powder immobilised enzyme this was 0.037 mg of enzyme per 24 mL of reaction volume, while for the enzyme immobilised in the monolith, it was 0.106 mg per 0.03 mL of reaction volume. Immobilising such a large amount of enzyme per unit reaction volume is virtually impossible with conventional batch reactor solutions. Only the use of flow-through microreactors, particularly of the packed bed and structural (monolithic) type, allows such a favourable ratio of surface area (on which the enzyme is deposited) to volume of the reaction mixture. Therefore this type of reactor is the focus of our review.

Even though large amounts of enzyme have a positive influence on the reaction, as shown above, it is important to investigate the limits thereof. The effect of the amount of enzyme and thus the suppression of diffusion limitations was the focus of Temporini *et al.*[157] and Zhang *et al.*[75] They immobilised different amounts of trypsin on the surface of silica monolithic columns[157] or pepsin on polymer monoliths.[75] It was found that when the amount of enzyme immobilised increased, there was an initial increase in activity, as expected. But further increases caused a drastic decrease in the enzyme activity. Those results indicate that either the high enzyme density on the solid support hinders access to the active site or the higher enzyme loading induces an aggregation and/or denaturation of the enzyme before or after immobilisation.

In the light of the above considerations, several factors can be identified that influence the kinetic parameters of enzymes embedded in the structure of monoliths. The first and foremost is the amount of enzyme immobilised. Initially, an increase in the amount of enzyme immobilised resulted in an increase in activity. This increase is however not unlimited. Once oversaturation occurs, a drastic decrease in activity was observed. Another factor is the correlation between the pore size of the monolith and the size of the substrate molecules. Fortunately, the pore size of the monolith has no significant effect on the kinetic parameters of processes using small-molecule substrates. For processes using macromolecular substrates, the pore size has a significant effect. Attention should also be paid to the chemical nature of the monolith surface

and the associated method of enzyme immobilisation. The influence of these parameters is ambiguous and must be determined on a case-by-case basis for individual enzyme–monolith pairs. From a chemical engineering point of view, the mode of operation of the monolith itself is also important. It allows a very favorable ratio of enzyme to reactant volume, which is reflected in the kinetic parameters.

4. Single- and two-phase reactions inside monoliths

The use of a biocatalyst immobilised on monolithic microreactors results in at least two phase processes: a liquid solution of substrates and an enzyme immobilised on a solid carrier. There are also situations where the reactants are in two different liquid phases, in which case the whole process should be considered as a three-phase process. In order to quantitatively describe these processes and their environmental impact, we will use factors such as space–time yield (STY) and environmental factor (EF). The STY is an important engineering parameter that determines the amount of product generated during a certain residence time in the reactor used, as well as the productivity of the reactor.[163] In turn, a significant parameter in the context of green chemistry assumptions is primarily the EF. This parameter makes it possible to determine the amount of waste generated in relation to the product produced.[164] Here we examine single- and two-phase liquid phase systems in the monolith reactor and give full STY and EF details, always where it was available.

Enzymes are mostly used in aqueous media, their natural environment. However, most biocatalysts also work well in organic solvents. Typically buffer saturated solvents are used as it has been shown that most enzymes require a minimal amount of water molecules to maintain their activity in a non-aqueous environment,[165] lipases being the exception.[166] This is important especially for the pharmaceutical industry, as most active compounds dissolve much better in organic solvents than in the aqueous phase. In some cases, the use of a monophasic organic medium effectively suppresses unwanted side reactions.[149,150] This suppression of unwanted side reactions can be achieved by using a suitable medium or, as in the case of microreactors, by reducing the process time, or more precisely, the contact time between the reactants and the catalyst. Achieving high substrate conversions in batch reactors typically requires several to tens of hours, whereas in a microreactor, the same effect can be achieved in a matter of seconds to tens of minutes, depending on the enzyme used and the type of reaction. This is due to the favourable ratio of enzyme covered surface area to reaction volume. This effect can be critical if an unwanted competing/side reaction is observed in the system. An example is the use of (*S*)-hydroxynitrile lyases from *Hevea brasiliensis* (*Hb*HNL) immobilised on a silica support in the (*S*)-mandelonitrile synthesis reaction carried out in a batch and continuous system.[149] In the batch system, 90% conversion was achieved after about 30 h, but the enantiomeric excess (ee) was only 40%. This low enantiomeric excess is due to the long contact time of the reactants with the support on which the enzyme is deposited, that is, the background reaction. By using a silica-structured microreactor, the contact time could be reduced to only about 20 min, resulting in high substrate conversion (~100%) and enantiomeric excess (ee ~ 100%). This effect has been confirmed in other work by the same team.[150] Furthermore, the use of monolithic flow microreactors significantly increases the STY compared to a batch system. For the monolithic microreactor with immobilised *Hb*HNL,[149] it was 613 g L^{-1} h^{-1} or after taking into account the amount of protein, it was 71 g L^{-1} h^{-1} $mg_{protein}^{-1}$, whereas in batch, it was ~2 g L^{-1} g^{-1} or 1 g L^{-1} h^{-1} $mg_{protein}^{-1}$. To date, many types of enzymes have been successfully immobilised on monolithic microreactors, conducting reactions in monophasic water or organic systems (Table 1). The main applications included enantioselective synthesis,[149,150,167,168] protein digestion[26] or demonstration of microreactor operation.[169]

The single phase processes are to date the most thoroughly investigated and optimised approach. Consequently, the EF here is typically particularly low. With EF below 1 for aqueous processes and 23 for synthesis in organic solvents, it shows the power of monolithic microreactors to achieve the green chemistry targets.

In the 1990s, non-aqueous solvents were extensively explored. With our current understanding of their influence on activity and stability, it is possible to achieve similar activities in organic solvents as in aqueous media. However, this often requires a higher degree of control.[171] Although the use of the biphasic reaction system (BRS) has been known since the last century (Pickering interfacial catalysis),[172,173] the trend of using BRS in enzymatic reactions carried out in a continuous system has only gained momentum in the last decade. BRS enables high substrate concentrations in the organic phase while saturating the aqueous layer.[174] Solutions in which the aqueous phase is made up of ionic liquids (ILs) are also successful.[165] One of the most commonly used groups of enzymes in this case are lipases, due to their interfacial activation, opening their hydrophobic cap that shields the active center.[166,175] In two-phase reactions, it is necessary to ensure intensive mixing[165,169] of the two phases, which is provided in monolithic microreactors due to their large reaction area.[176] The use of monolithic microreactors in a biphasic system allows for increased enantioselectivity and STY (up to 28 $g_{product}$ L^{-1} h^{-1} in flow compared to 0.7 $g_{product}$ L^{-1} h^{-1} in the batch system) in kinetic resolution processes.[177] Enzymatic chemical processes in a multiphase system are primarily successful in biorefinery[178,179] and pharmaceutical drug synthesis.[180] They represent a green way to synthesize pharmaceuticals and chemical compounds according to the sustainable chemical industry principles.[180]

The two-phase reactions are not limited to aqueous–organic systems but include also liquid–gas systems. Efficient gas dosing into monolithic microreactors is an extremely difficult issue due to their wall structure. Recently, an innovative solution has emerged for the use of a monolithic microreactor

Table 1 Monolithic microreactors' application in processes where reactants are in single phase, aqueous or organic solvents

Monolith type	Enzyme	Immobilisation technique	Biocatalysis result	Application	EF [g_{waste} $g_{product}^{-1}$]	STY [$g_{product}$ L^{-1} h^{-1}]	Ref.
Silica porous monolith obtained by the sol–gel method	HNLs (*At*HNL, *Me*HNL, *Hb*HNL)	Covalent binding *via* amino or epoxide groups	Higher STY yield and enantioselectivity compared to the batch system	Highly enantioselective chiral cyanohydrin synthesis	22.95	*At*: 1290; *Me*: 1235; *Hb*: 613	149 and 150
		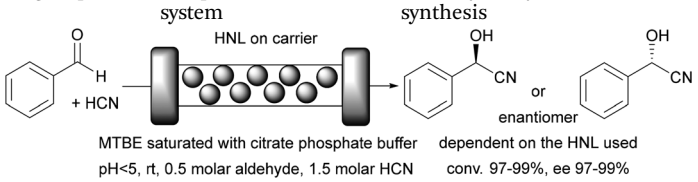					
	Trypsin	Covalent binding *via* amino, cyano or epoxide groups	High practical potential in protein proteolysis without any earlier pretreatment	Protein digestion	n.a.	n.a.	26, 39 and 157
	Invertase	Covalent binding *via* amino groups	1000 times faster sucrose hydrolysis than in the batch system	Proof of concept of applying a monolith microreactor	0.29	6009	56
		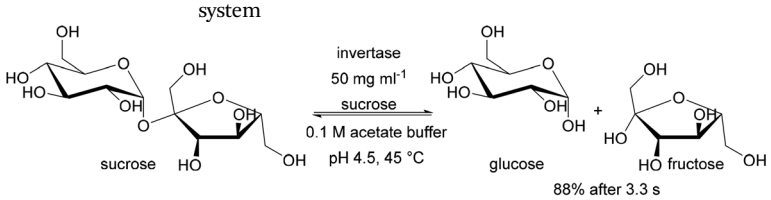					
Alginate–silica hybrid	β-Glucosidase	Cross-linking	High *p*NPG hydrolysis yield, 94% after 24 h	Obtaining saponins from plant materials and scaffolds for tissues	0.59	1.34	167
		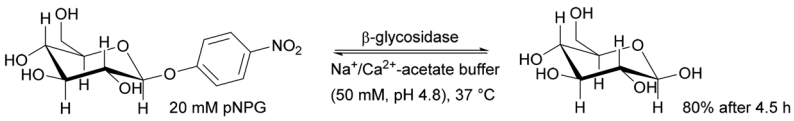					
Monolith coated with polyaniline	Penicillin G acylase (PenGA)	Cross-linking	95% of original activity maintained after 48 h of continuous operation	Semisynthetic penicillin production	0.23	17.39	170
		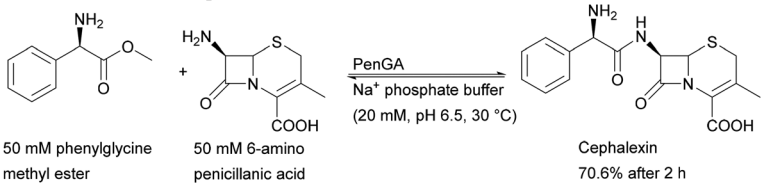					
Poly(vinyl alcohol) monolith functionalised *via* reacting glutaraldehyde and polyethylenimine	Lipase, HRP	Covalent binding *via* aldehyde groups	Higher activity and stability of immobilised enzymes compared to their free form	Biotechnology and biomedical fields' potential applications	n.a.	n.a.	168

HRP, horse radish peroxidase; *p*NPG, 4-nitrophenyl-β-D-glucopyranoside.

enclosed by a semi-permeable wall, capable of continuously and efficiently dosing oxygen. This allows the system to achieve operational stability for a minimum of 40 h.[181] A summary of the application of a biphasic reaction system in monolithic reactors is presented in Table 2 and Fig. 5.

The two-phase processes are in many cases still in a development stage. Therefore, reliable calculations of EF and STY are often not possible. The example of *Ms*AcT in an aqueous organic system does however also indicate the potential to achieve the green chemistry principles.

Table 2 Monolithic microreactors' application in processes where reactants are in two phases

Monolith type	Immobilisation technique	Biocatalysis result	Application	EF [g_{waste} $g_{product}^{-1}$]	STY [$g_{product}$ L^{-1} h^{-1}]	Ref.
Silica porous monolith obtained by the sol–gel method	Covalent binding *via* amino groups and transition metals	Full and rapid (in a minute) transesterification	Transesterification of neopentylglycol	7.62	820	174
	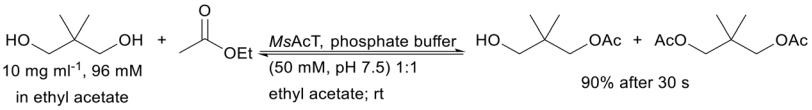					
	Physical adsorption *via* multipoint interactions between the enzyme and the carrier surface	High productivities in the hydrolysis of 4-NPB in media: Tris-HCl buffer and decane solvent	Proof of higher activity in immobilised enzymes compared to free enzymes	4294	1042	175
	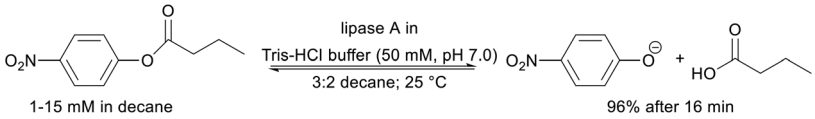					
Acrylamide porous monolith	Encapsulation and cross-linking	Specific activity above 90% in 15 cycles	Development of a system to efficiently immobilise enzymes and perform reactions	282	19 241	176
	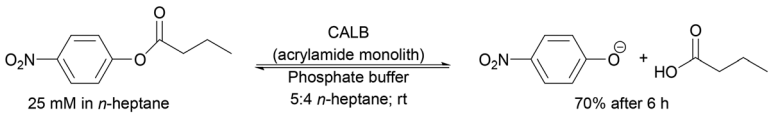					
Hybrid polyurethane monolith with cellulase microbeads	Encapsulation and cross-linking	Higher productivities compared to batch-type reactions	Creation of an efficient system for chiral ester and amide synthesis	n.a.	5	177
	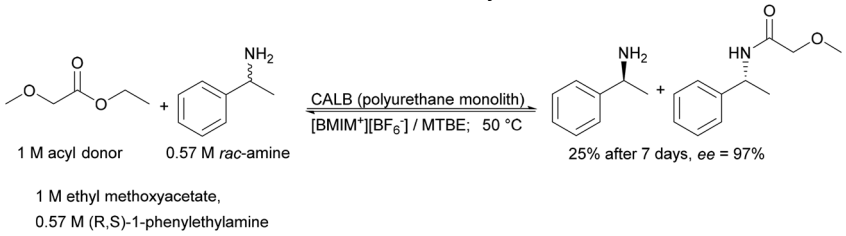					
Hybrid polymeric monoliths: from styrene or acrylate, supported with ILs	Covalently supported IL phase with an absorbed enzyme solution	The best results were obtained with the most hydrophobic monolith	Synthesis of citronellal propionate in supercritical carbon dioxide by transesterification	n.a.	20	182
	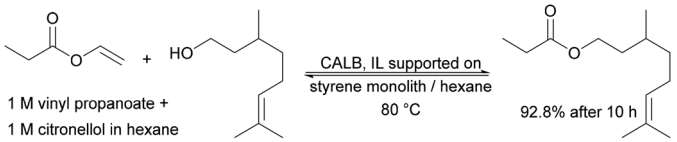					
Thiolene monolith with PDMS wall	Adsorption *via* thiol groups	40 h operational stability with diffused oxygen supply	Alternative approach for efficient enzymatic synthesis with continuous gas delivery	n.a.	n.a.	181
	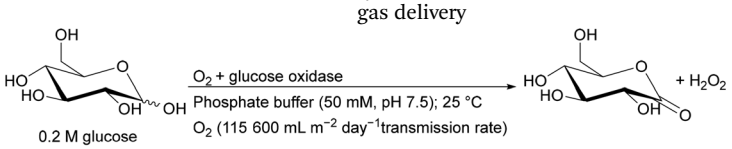					

CALB, lipase B from *Candida antarctica*; *Ms*AcT, acyltransferase; PDMS, polydimethylsiloxane.

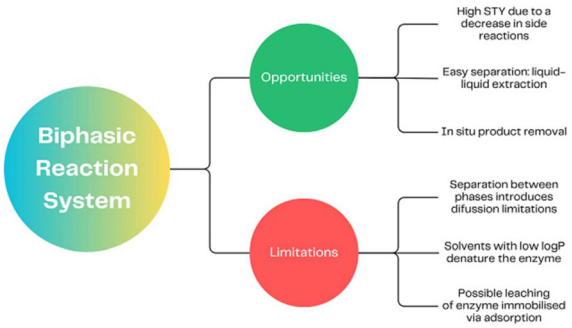

Fig. 5 Opportunities and limitations in biphasic reaction system applications.

5. Reaction cascades in monoliths

Multi-enzymatic cascade reactions have become very popular in recent years and represent a promising route to the production of pharmaceuticals, cosmetics, biofuels or fine chemicals.[183,184] In contrast to classical multi-step synthesis, multi-enzymatic cascade reactions eliminate the need to isolate and purify intermediates after each step, thus reducing the number of steps and DSP. This saves time, reduces the amount of solvent used and therefore generates less waste, reducing the environmental and economic costs while at the same time helping to implement the principles of green chemistry. In many cases, higher yields are also achieved because, in cascade systems, the product formed in one step is rapidly consumed in the next, so the balance of the enzymatic reaction can be shifted towards the product, avoiding the need for excess reactants.[156] In addition, the immobilisation of multiple enzymes enables the use of cascade processes in industry. Multiple enzyme immobilisation can be achieved by immobilising individual enzymes on a separate support or by co-immobilising all enzymes on a single support (Fig. 6). The advantage of the former is undoubtedly the flexibility of unit operation and the ability to determine the activity and stability of each immobilised enzyme, which is unfortunately very difficult for co-immobilised enzymes. However, co-immobilisation of enzymes reduces or eliminates the lag time, which can contribute to increased reaction rates and catalytic efficiency. This lag occurs when several enzymes are immobilised on separate supports and is due to the fact that the concentration of intermediates is initially low, preventing subsequent enzymes in the reaction chain from showing activity at the beginning of the reaction. Co-immobilisation of enzymes also removes the diffusion limitations in the transfer of intermediates from the active site of the first enzyme to the second, which is the case when immobilised on separate supports. However, when immobilising several enzymes on a single support, it is not only the enzyme/support interactions that are significant, but also the properties of the different enzymes. It is extremely important to find optimal conditions (temperature, pH and reaction medium) where all the enzymes involved in the cascade show high activity and stability. In the case of independently immobilised enzymes, a different, specifically optimised immobilisation protocol can be used for each enzyme, the most appropriate support and its modification (*e.g.*, a functional group on the support).[185,186]

5.1 Cascades in one monolith

One of the variants of the multienzyme cascade processes is a single reactor system, where all enzymes are immobilised on

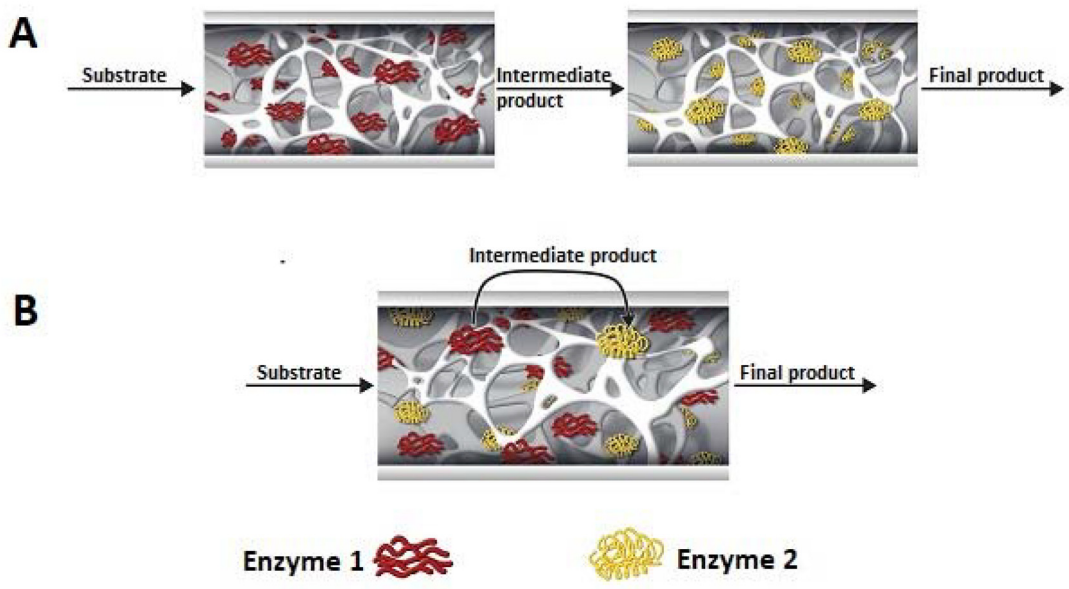

Fig. 6 Classification of multienzyme cascade reactions in monoliths in flow: catalysed by a sequential immobilised enzyme system (stepwise) (A) and catalysed by a co-immobilised one-monolith enzyme system (B).

the same monolith. Co-immobilising enzymes is greatly facilitated by the use of the same immobilisation conditions for each biocatalyst as well as the same range of temperature and pH optimum of enzymes subjected to the co-immobilisation process. Meeting these conditions is necessary to obtain the most efficient co-immobilised multi-enzymatic system possible. Recent reports on the use of co-immobilised multienzyme systems on monolithic carriers mainly refer to the co-immobilisation of oxidoreductases and lyases. A summary of the application of co-immobilised multienzymatic monolithic reactors is presented in Table 3.

An interesting example demonstrating the superiority of using a two-enzyme system in a single monolith is the cascade created by citrate lyase (CL) and malate dehydrogenase (MDH). Initially, the enzymes were immobilised separately and worked in a sequential arrangement of CL and the following MDH. For its catalytic activity, CL requires Mg^{2+} ions. This can however also form a complex with the product of the reaction that inhibits the enzyme CL. The use of sequential immobilisation promoted the formation of this complex and inhibited the process. Only the embedding of both enzymes in one monolith allowed immediate transformation of the product, significantly improving the stability of CL.[187] Monoliths based on the silica skeleton have found applications in the construction of heterogeneous enzyme systems using dendronised polymer–enzyme conjugates. This solution allowed for the reproducible immobilisation of predetermined amounts of catalytically active enzyme molecules.

Recently, such a system has been used for immobilisation of horseradish peroxidase isoenzyme C (HRP) and bovine erythrocyte carbonic anhydrase (BCA) and has been tested as a heterogeneous biocatalyst in a one-monolith cascade reaction with co-immobilised enzymes and two bioreactors in a sequential system in 2′,7′-dichlorofluorescein synthesis. For both reactor systems, the final product formation was the same with 30 μM hydrogen peroxide (co-substrate). However, the application of 10 μM H_2O_2 shows about 20% higher product formation with co-immobilised enzymes.[55] This clearly indicated a higher reaction efficiency when the co-immobilisation system is used, which additionally shortens the delay time even if lower substrate concentrations are used.

Table 3 Co-immobilised multi-enzymatic monolithic bioreactors

Immobilised enzymes	Monolith type	Application	Ref.
Citrate lyase + malate dehydrogenase	CIM disk – commercial polymethacrylate monolithic column functionalised with epoxide groups	Indirect analysis of citrate	187
Horseradish peroxidase + glucose oxidase	pH-responsive polymethacrylate monolithic capillary grafted with poly(4-vinylphenylboronic acid)	Glucose detection, obtaining reusable biosensors	188
Trypsin + chymotrypsin	Chromolith column – commercial monolithic silica column functionalised with epoxide groups	Protein digestion	189
Horseradish peroxidase + bovine carbonic anhydrase	Silica monolith with a dendronized polymer–enzyme conjugate	Controllable immobilisation method application	55
Invertase + glucose oxidase + horseradish peroxidase	Lab-made polymethacrylate monolithic capillary column grafted with vinyl azlactone	Directional multienzymatic reactions	190

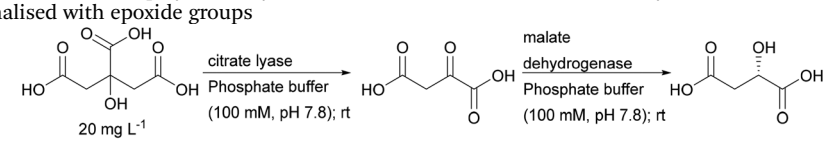

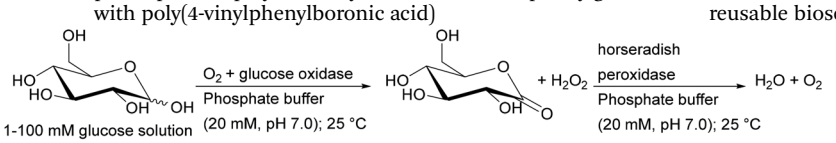

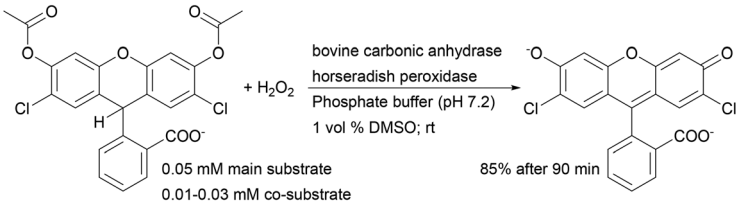

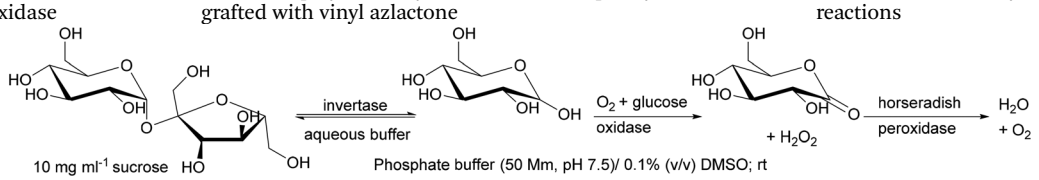

An interesting example is the co-immobilisation of invertase (INV), glucose oxidase (GOX) and HRP inside a polymeric monolith structure within microfluidic devices by photo-patterning. The enzymes were co-immobilised in different orders of occurrence in the monolith, which was made possible by the use of photo-patterned vinyl azlactone grafting, through which immobilisation occurred. The first step of the reaction was the hydrolysis of sucrose (first substrate) to glucose and fructose catalysed by INV, then GOX oxidises glucose to gluconolactone and hydrogen peroxide, which was further used by HRP to oxidise Amplex Red (second substrate) to fluorescent resorufin. The authors established that only the sequence of co-immobilised enzymes INV-GOX-HRB gave high product yield.[190] This demonstrates how important not only the close contact of enzymes involved in the cascade but also placing the co-immobilised biocatalysts in the correct order on the monolith (if possible) is to control the reaction sequence.

All of these examples are proof of principle to solve a given problem (product inhibition, order of immobilisation) that were not directed towards high productivity and therefore no meaningful EF or STY could be calculated.

5.2 Monoliths with separate reactions in a row/parallel

The second possibility for the multienzyme cascade processes is to link multiple microreactor (monolithic) systems, where each enzyme is immobilised on a separate monolith under optimal conditions and can be applied at different reaction parameters (Fig. 6A). The advantages of separate immobilisation of enzymes on individual monoliths are the availability of a single reactant that can be used either independently or in various combinations in sequence as well as separate replacements once the individual enzymes lose activity. A summary of the application of sequential multienzyme monolithic reactors is presented in Table 4.

The importance of the order of using a single-enzyme microreactor in a multienzyme sequential cascade was demonstrated in studies on the enzymatic digestion of genomic DNA. Three enzymes – deoxyribonuclease I (DNase I), snake venom phosphodiesterase (SVP), and alkaline phosphatase (ALPase) – were constructed in cascade bioreactors assembled by tandem connection (DNase I – SVP – ALPase) on silica-based capillary monoliths. The developed solution is promising in highly sensitive detection and rapid identification of adducts in genomic DNA samples. The correct connection of the bioreactor sequence has an influence on the digestion performance. Removing the SVP bioreactor or placing it before the cascade (instead of the DNase I bioreactor) reduced the digestion efficiency from 99.3% to 59.8–83.7%.[191] Both DNase I and SVP are capable of generating mononucleotides, but DNase I tends to digest double-stranded DNA to generate small DNA fragments. Thus, combining with DNase I at the outset provided a high yield of genomic DNA digestion. The authors of this study succeeded in developing a system that contained benzonase endonuclease instead of DNase I, resulting in a reduction in genomic DNA digestion time from 45 to 10 minutes.[192] Stability tests showed less than 20% variation of enzyme activity when the immobilised bioreactor was stored in Tris-HCl buffer (10 mM, pH 7.4) at 4 °C for 30 days. As expected from earlier data,[134–138,144–146] the free enzyme solution mixture, stored under the same conditions, lost its activity within 1 day. Therefore, the cascade monolithic bioreactors have an advantage in terms of stability and reusability. A direct comparison of immobilised enzymes for batch and in a monolith is given above (Table 1), displaying advanced reactivity and stability for the monolith.

Monolith microreactors were also employed for the synthesis of APIs or pharmaceutical intermediates. Purine nucleoside phosphorylase from *Aeromonas hydrophila* (*Ah*PNP) was earlier covalently immobilised on a silica particle based support, which caused a high backpressure resulting in a loss of enzyme activity.[194] Two years later, a study was published that used a cascade reaction with immobilised uridine phosphorylase from *Clostridium perfringens* (*Cp*UP) on a commercial Chromolith Flash monolithic support. This allowed reducing the back-pressure and obtaining the desired nucleoside products.[195] The co-immobilised *Cp*UP and *Ah*PNP on one monolith support in a one-reactor system provided 84% conversion over 120 min in flow (0.5 ml min^{-1}) reaction for the synthesis of 2′-deoxyadenosine.[193] However, the step-by-step two bioreactor system approached 95% conversion yield after 90 min reaction with the same flow.[195] Co-immobilised systems mimic the "one-pot" transglycosylation system involving two enzymes, but independent bioreactors turned out to be better for controlling the multienzyme reaction.

Heterogeneous multienzyme systems have applications, especially in sugar synthesis and transformation of sugar derivatives. Traditional chemical pathways to sugars usually suffer from poor stereoselectivity and the downstream processes and purification of intermediate products are difficult. Several multienzyme systems suitable for sugar coupling systems have been found. An excellent example is the enzymatic synthesis of trehalose catalysed by UDP-glucose pyrophosphorylase from *Thermocrispum agreste* (*Ta*GalU) and trehalose transferase from *Thermoproteus uzoniensis* (mCherry-*Tu*TreT) immobilised on monolithic silica supports in two variants: co-immobilisation and step-by-step synthesis. Significant differences in temperature requirements affected both the activity and stability of each immobilised enzyme, preventing both reactions from occurring simultaneously in one microreactor. Thus, the application of a sequential cascade allowed the reaction to be carried out in separate monoliths, maintaining ideal temperature conditions for each enzyme, allowing the highest activity for each of the immobilised biocatalysts. Under optimised conditions, the productivity values varied, depending on the applied flow rate, from 1.9 to 14.4 g UDP-glucose per L per h per $mg_{protein}$ obtained by immobilised *Ta*GalU and 8.3 to 49.6 g trehalose per L per h per $mg_{protein}$ obtained by immobilised mCherry-*Tu*TreT.[57]

The latter examples have excellent EF (1.42 and 5.18) and STY, again demonstrating the power of flow chemistry to achieve the green chemistry principles.

Table 4 Sequential multi-enzymatic monolithic bioreactors

Monolith type	Application	EF [g_{waste} $g_{product}^{-1}$]	STY [$g_{product}$ L^{-1} h^{-1}]	Ref.
Silica based capillary monolith functionalised *via* amino groups using glutaraldehyde as a cross-linking agent	Digestion of genomic DNA, analysis and identification of structural DNA modifications	n.a.	n.a.	191 and 192
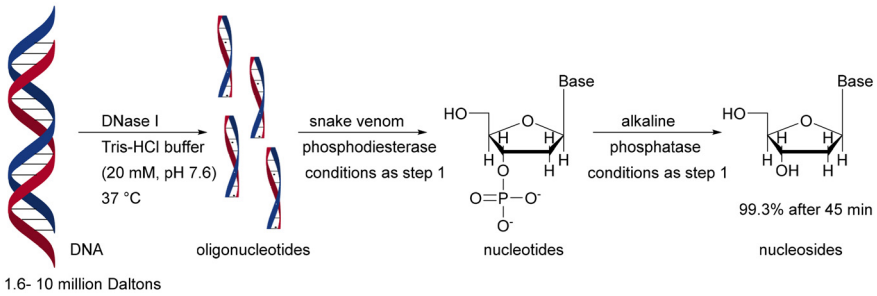				
Chromolith flash silica support	Synthesis of arabinosyladenine, an antiviral nucleoside	1.42	4.32	193
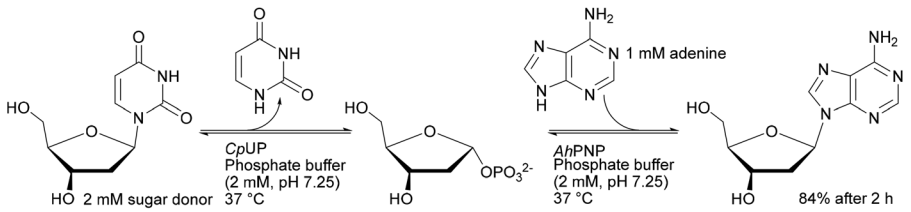				
Lab-made silica monoliths functionalised *via* amino groups	Trehalose synthesis, transformation of sugar derivatives	5.18	I step: 12–91 II step: 12–70	156
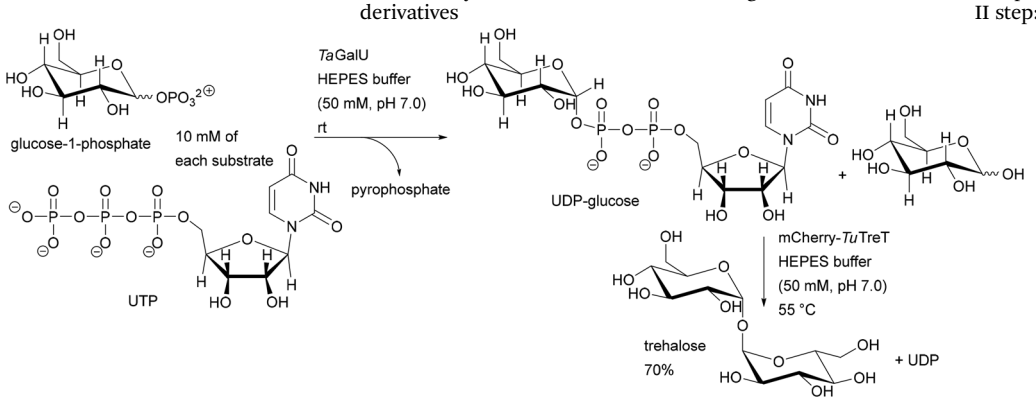				

*Ah*PNP, purine nucleoside phosphorylase; *Cp*UP, uridine phosphorylase; mCherry-*Tu*TreT, trehalose transferase; *Ta*GalU, UDP-glucose pyrophosphorylase

5.3 Cofactors and considerations concerning them

The selective syntheses catalysed by enzymes are very versatile and straightforward to perform. However, a wide range of enzymes requires a cofactor. This can be a metal or an organic cofactor such as thiamine or Fe-containing porphyrins. These cofactors are tightly bound to the enzyme and need to be replenished only occasionally. Therefore they do not need to be taken into consideration during enzyme immobilisation. For redox enzymes, the cofactor, especially nicotinamide adenine dinucleotide (NADH) and its phosphorylated form (NADPH), needs to be regenerated. This is particularly important when considering industrial scale processes and has to date been solved for batch processes. There are a number of methods for regenerating cofactors[4,196,197] *i.e.* enzymatic, chemical, electrochemical or photocatalytic. Of the methods listed here, those using enzymes are the most popular. The use of isolated enzymes rather than whole cells allows much better process control and we will focus on this approach. Two main strategies for cofactor regeneration are known (Fig. 7). In the easiest case, found mainly for alcohol dehydrogenases (ADH), a 'coupled substrate' allows the application of a single enzyme that catalyses both substrate conversion and cofactor regeneration. The cofactor does not leave the active site and the same considerations as for the cofactors like thiamine apply. In the case of ADHs, high concentrations of the sacrificial substrate are necessary to drive the equilibrium toward the desired product. While straightforward, this in turn leads to a loss of activity in

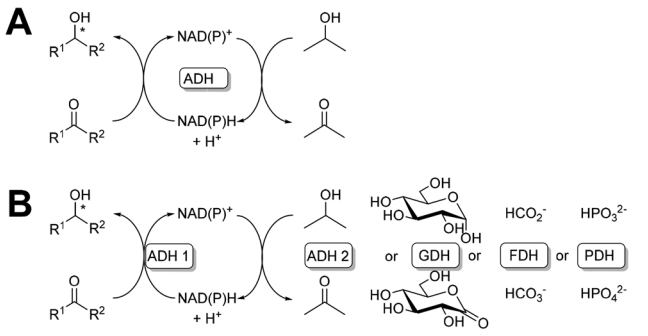

Fig. 7 Schematic representation of cofactor enzymatic regeneration: a coupled substrate system (A) and a coupled enzyme system (B).

the main target reaction as a result of competition among substrates and cosubstrates for the same active site on the ADH.[198] The 'coupled enzyme' involves the use of two enzymes, the first to produce the main product and the second to regenerate a cofactor with the production of a by-product. The by-product is typically chosen to ensure an irreversible reaction and thus maximal driving force and optimal yields in the desired reaction. Clearly here the cofactor has to be mobile and its immobilisation has to be considered separately.

Combining oxidation and reduction in a cascade leads to economical and efficient transformation. This is why co-immobilisation is so eagerly used to design multienzyme cascade systems for cofactor recycling. It allows us to obtain self-sufficient heterogeneous biocatalysts that do not require exogenous cofactor delivery.[199,200]

A novel micromonolith bioreactor with co-immobilised ADH from *Thermoanaerobacter brockii* (*Tb*SADH) and NADP(H) has been recently developed to provide a cost-effective basis for cofactor-dependent biocatalysis.[201] The cell extract with *Tb*SADH was cross-linked by a hydrogel (cEAG) and then the cofactor was cross-linked to form a NADP@cEAG monolithic microreactor. There is no need to leave the active site of the enzyme to fully regenerate the cofactor during the catalytic cycle (Fig. 7A). The microreactor with a heterogeneous biocatalyst and cofactor was characterized by high enantioselectivity (<99%) and a high STY of 46.3 g L^{-1} h^{-1} with 94.8% conversion in the flow synthesis of (*R*)-1-phenylethanol at 0.01 ml min^{-1} flow rate, which indicates the unique advantage of co-immobilisation on monolith microreactors in recycling cofactors in flow. The additional co-substrate was isopropanol, which did not generate a significant increase in the process costs.

Application of a coupled enzyme system in cofactor regeneration was tested in an enzymatic reaction for the synthesis of formate from carbon dioxide gas in a tandem reaction. The production enzyme was a high-performance formate dehydrogenase from *Methylobacterium extorquens* AM1 (*Me*FDH1), while the regeneration of NADH was performed by phosphite dehydrogenase from *Pseudomonas stutzeri* (*Ps*PDH). Both enzymes and cofactors were immobilised by cross-linking with poly(ethylene glycol) diglycidyl ether (PEGDGE) on hierarchical porous inorganic monoliths, from silica or carbon. This allowed the fabrication of a system of two heterogeneous biocatalysts with a flexibly bound cofactor capable of moving between active centers for regeneration[6] (Fig. 7B). After testing, this carbon monolithic reactor proved superior to achieve the highest productivity reported to date for NAD-dependent biocatalytic systems for producing formate from carbon dioxide gas without the need for additional hydrogenation and under atmospheric conditions.[202]

The immobilisation of cofactors for the coupled enzyme approach and their effective recovery through their reuse[203,204] is a prerequisite for the economic application of these enzymes. However, immobilised cofactors may have lower availability than free cofactors dissolved in the reaction mixture. This is as a result of slower mass transfer, which must be compensated by the cofactor recycling and reuse.[198] Both ionic and covalent immobilisation have been studied. At low buffer strengths, ionic immobilisation on ionic carriers has been successful. Permanent binding of cofactors with long-lasting activity is still a challenge. The use of encapsulation leads to rapid leaching of the cofactor in the reaction solution.[205] One way to improve stability is to link the cofactor to another macromolecule (*e.g.* dextran,[206] chitosan[207]) *via* a permanent covalent bond. Noncovalent attachment of NAD^+ on carbon nanotubes[208] or covalent binding of NAD^+ *via* epoxy groups to the surface of a silica matrix obtained by the sol–gel method has also been proposed.[205] However, permanent binding of cofactors on monoliths is still a relatively new topic, with challenging research questions[209,210] and solutions.

6 Conclusions

To summarise the above discussion from a green chemistry perspective, biocatalysis in a continuous flow system carried out in monolithic microreactors fulfils most of the principles of green chemistry. The high selectivity of enzymes ensures that virtually no side-products are formed and thus no waste is generated. The combination of biocatalysis and flow chemistry additionally minimises energy consumption by intensifying mass and heat exchange. In addition, flow chemistry in monolithic microreactors allows for a significant reduction in reaction volume while maintaining a high efficiency of the process carried out. As exemplified in Table 1 for the conversion of benzaldehyde with hydrogen cyanide[149] and in Table 2 for transesterifications,[174] the residence time in a monolithic microreactor at which near 100% conversion and enantioselectivity is achieved is often less than a few minutes. While biocatalysis in flow is not yet fully applicable on an industrial scale, its potential for accelerating the use of enzymes towards green chemistry principles is obvious.

Author contributions

AL, KS and UH wrote the review. Together they edited and designed the structure of the review.

Data availability

This is a review; therefore, we do not have any data except for the references in the manuscript.

Conflicts of interest

There are no conflicts to declare.

Acknowledgements

The authors are grateful for generous financial support from the European Union's European Innovation Council programme under grant agreement 101136310 (cassaFLOW for U. H.) and from the Ministry of Education and Science (Poland) programme under grant agreement PN/01/0267/2022 (The Pearls of Science for A. L.).

References

1 A. R. Alcántara, P. Domínguez de María, J. A. Littlechild, M. Schürmann, R. A. Sheldon and R. Wohlgemuth, *ChemSusChem*, 2022, **15**, e202102709.
2 C. K. Winkler, J. H. Schrittwieser and W. Kroutil, *ACS Cent. Sci.*, 2021, **7**, 55–71.
3 S. Wu, R. Snajdrova, J. C. Moore, K. Baldenius and U. T. Bornscheuer, *Angew. Chem., Int. Ed.*, 2021, **60**, 88–119.
4 U. Hanefeld, F. Hollmann and C. E. Paul, *Chem. Soc. Rev.*, 2022, **51**, 594–627.
5 J. A. McIntosh, T. Benkovics, S. M. Silverman, M. A. Huffman, J. Kong, P. E. Maligres, T. Itoh, H. Yang, D. Verma, W. Pan, H. I. Ho, J. Vroom, A. M. Knight, J. A. Hurtak, A. Klapars, A. Fryszkowska, W. J. Morris, N. A. Strotman, G. S. Murphy, K. M. Maloney and P. S. Fier, *ACS Cent. Sci.*, 2021, **7**, 1980–1985.
6 J. Coloma, Y. Guiavarc'h, P. L. Hagedoorn and U. Hanefeld, *Chem. Commun.*, 2021, **57**, 11416–11428.
7 R. DiCosimo, J. McAuliffe, A. J. Poulose and G. Bohlmann, *Chem. Soc. Rev.*, 2013, **42**, 6437–6474.
8 S. C. Cosgrove and A. P. Mattey, *Chem. – Eur. J.*, 2022, **28**, e202103607.
9 A. Naramittanakul, S. Buttranon, A. Petchsuk, P. Chaiyen and N. Weeranoppanant, *React. Chem. Eng.*, 2021, **6**, 1771–1790.
10 T. Sokač Cvetnić, A. Šalić, M. Benković, T. Jurina, D. Valinger, J. Gajdoš Kljusurić, B. Zelić and A. Jurinjak Tušek, *Catalysts*, 2023, **13**, 708.
11 Y. J. Hu, J. Chen, Y. Q. Wang, N. Zhu, Z. Fang, J. H. Xu and K. Guo, *Chem. Eng. J.*, 2022, **437**, 135400.
12 M. B. Ansorge-Schumacher and O. Thum, *Chem. Soc. Rev.*, 2013, **42**, 6475–6490.
13 Y. Asano, S. Togashi, H. Tsudome and S. Murakami, *Pharm. Eng.*, 2010, **30**, 1–9.
14 J. M. Woodley and N. J. Titchener-Hooker, *Bioprocess Eng.*, 1996, **14**, 263–268.
15 R. Wohlgemuth, I. Plazl, P. Žnidaršič-Plazl, K. V. Gernaey and J. M. Woodley, *Trends Biotechnol.*, 2015, **33**, 302–314.
16 Z. Tang, Y. Oku and T. Matsuda, *Org. Process Res. Dev.*, 2024, **28**, 1308–1326.
17 P. Žnidaršič-Plazl, *Biotechnol. J.*, 2019, **14**, 1800580.
18 D. Pirozzi, M. Abagnale, L. Minieri, P. Pernice and A. Aronne, *Chem. Eng. J.*, 2016, **306**, 1010–1016.
19 K. S. Elvira, X. C. I. Solvas, R. C. R. Wootton and A. J. deMello, *Nat. Chem.*, 2013, **5**, 905–915.
20 A. deMello and R. Wootton, *Lab Chip*, 2002, **2**, 7–13.
21 J. Lawrence, B. O'Sullivan, G. J. Lye, R. Wohlgemuth and N. Szita, *J. Mol. Catal. B: Enzym.*, 2013, **95**, 111–117.
22 H. Kim, A. Nagaki and J. I. Yoshida, *Nat. Commun.*, 2011, **2**, 264.
23 J. González-Álvarez, P. Arias-Abrodo, M. Puerto, M. E. Viguri, J. Perez and M. D. Gutiérrez-Álvarez, *New J. Chem.*, 2015, **39**, 8560–8568.
24 A. Abdul Halim, N. Szita and F. Baganz, *J. Biotechnol.*, 2013, **168**, 567–575.
25 M. Oelschlägel, A. Riedel, A. Zniszczoł, K. Szymańska, A. B. Jarzębski, M. Schlömann and D. Tischler, *J. Biotechnol.*, 2014, **174**, 7–13.
26 K. Szymańska, M. Pietrowska, J. Kocurek, K. Maresz, A. Koreniuk, J. Mrowiec-Białoń, P. Widłak, E. Magner and A. Jarzębski, *Chem. Eng. J.*, 2016, **287**, 148–154.
27 K. Szymańska, A. Ciemięga, K. Maresz, W. Pudło, J. Malinowski, J. Mrowiec-Białoń and A. B. Jarzębski, *Front. Chem. Eng.*, 2021, **3**, 1–14.
28 A. Adamo, R. L. Beingessner, M. Behnam, J. Chen, T. F. Jamison, K. F. Jensen, J. C. M. Monbaliu, A. S. Myerson, E. M. Revalor, D. R. Snead, T. Stelzer, N. Weeranoppanant, S. Y. Wong and P. Zhang, *Science*, 2016, **352**, 61–67.
29 T. A. Nijhuis, A. E. W. Beers, T. Vergunst, I. Hoek, F. Kapteijn and J. A. Moulijn, *Catal. Rev. - Sci. Eng.*, 2001, **43**, 345–380.
30 J. L. Williams, *Catal. Today*, 2001, **69**, 3–9.
31 C. Yao, L. Qi, W. Hu, F. Wang and G. Yang, *Anal. Chim. Acta*, 2011, **692**, 131–137.
32 Y. Liang, D. Tao, J. Ma, L. Sun, Z. Liang, L. Zhang and Y. Zhang, *J. Chromatogr. A*, 2011, **1218**, 2898–2905.
33 S. Wu, L. Sun, J. Ma, K. Yang, Z. Liang, L. Zhang and Y. Zhang, *Talanta*, 2011, **83**, 1748–1753.
34 A. Sachse, A. Galarneau, F. Di Renzo, F. Fajula and B. Coq, *Chem. Mater.*, 2010, **22**, 4123–4125.
35 A. Koreniuk, K. Maresz and J. Mrowiec-Białoń, *Catal. Commun.*, 2015, **64**, 48–51.
36 A. Sachse, A. Galarneau, F. Fajula, F. Di Renzo, P. Creux and B. Coq, *Microporous Mesoporous Mater.*, 2011, **140**, 58–68.
37 A. Koreniuk, K. Maresz, K. Odrozek and J. Mrowiec-Białoń, *Microporous Mesoporous Mater.*, 2016, **229**, 98–105.

38 A. Galarneau, A. Sachse, B. Said, C. H. Pelisson, P. Boscaro, N. Brun, L. Courtheoux, N. Olivi-Tran, B. Coasne and F. Fajula, *C. R. Chim.*, 2016, **19**, 231–247.
39 J. Ma, Z. Liang, X. Qiao, Q. Deng, D. Tao, L. Zhang and Y. Zhang, *Anal. Chem.*, 2008, **80**, 2949–2956.
40 P. Yang, T. Deng, D. Zhao, P. Feng, D. Pine, B. F. Chmelka, G. M. Whitesides and G. D. Stucky, *Science*, 1998, **282**, 2244–2246.
41 C. G. Oh, Y. K. Baek and S. K. Ihm, *Adv. Mater.*, 2005, **17**, 270–273.
42 M. Antonietti, B. Berton, C. Göltner and H. P. Hentze, *Adv. Mater.*, 1998, **10**, 154–159.
43 Q. Luo, L. Li, B. Yang and D. Zhao, *Chem. Lett.*, 2000, **29**, 378–379.
44 Y. Shin, L. Wang, J. H. Chang, W. D. Samuels and G. J. Exarhos, *Stud. Surf. Sci. Catal.*, 2003, **146**, 447–451.
45 K. Nakanishi, *J. Porous Mater.*, 1997, **4**, 67–112.
46 K. Nakanishi, H. Minakuchi, N. Soga and N. Tanaka, *J. Sol-Gel Sci. Technol.*, 1997, **8**, 547–552.
47 R. Takahashi, K. Nakanishi and N. Soga, *J. Non-Cryst. Solids*, 1995, **189**, 66–76.
48 K. Nakanishi, *J. Sol-Gel Sci. Technol.*, 2000, **19**, 65–70.
49 K. Nakanishi, Y. Sato, Y. Ruyat and K. Hirao, *J. Sol-Gel Sci. Technol.*, 2003, **26**, 567–570.
50 J. H. Smått, S. Schunk and M. Lindén, *Chem. Mater.*, 2003, **15**, 2354–2361.
51 A. Ciemięga, K. Maresz and J. Mrowiec-Białoń, *Appl. Catal., A*, 2018, **560**, 111–118.
52 A. Ciemięga, K. Maresz and J. Mrowiec-Białoń, *Microporous Mesoporous Mater.*, 2017, **252**, 140–145.
53 K. Maresz, A. Ciemięga and J. Mrowiec-Białoń, *Chem. Eng. J.*, 2020, **379**, 122281.
54 N. Ghéczy, S. Tao, S. Pour-Esmaeil, K. Szymańska, A. B. Jarzębski and P. Walde, *Macromol. Biosci.*, 2023, **23**, 1–20.
55 N. Ghéczy, W. Xu, K. Szymańska, A. B. Jarzębski and P. Walde, *ACS Omega*, 2022, **7**, 26610–26631.
56 K. Szymańska, W. Pudło, J. Mrowiec-Białoń, A. Czardybon, J. Kocurek and A. B. Jarzębski, *Microporous Mesoporous Mater.*, 2013, **170**, 75–82.
57 D. Kowalczykiewicz, M. Przypis, L. Mestrom, A. Kumpf, D. Tischler, P. L. Hagedoorn, U. Hanefeld, A. Jarzębski and K. Szymańska, *Chem. Eng. J.*, 2022, **427**, 1–8.
58 H. Minakuchi, K. Nakanishi, N. Soga, N. Ishizuka and N. Tanaka, *Anal. Chem.*, 1996, **68**, 3498–3501.
59 N. Ishizuka, H. Minakuchi, K. Nakanishi, N. Soga and N. Tanaka, *J. Chromatogr. A*, 1998, **797**, 133–137.
60 M. Kozakiewicz-Latała, D. Marciniak, K. Krajewska, A. Złocińska, K. Prusik, B. Karolewicz, K. P. Nartowski and W. Pudło, *Mol. Pharm.*, 2023, **20**, 641–649.
61 W. Pudło, P. Borys, G. Huszcza, A. Staniak and R. Zakrzewska, *Eur. J. Pharm. Biopharm.*, 2019, **141**, 12–20.
62 G. Hasegawa, K. Kanamori, T. Kiyomura, H. Kurata, T. Abe and K. Nakanishi, *Chem. Mater.*, 2016, **28**, 3944–3950.
63 B. Luangon, A. Siyasukh, P. Winayanuwattikun, W. Tanthapanichakoon and N. Tonanon, *J. Mol. Catal. B: Enzym.*, 2012, **75**, 80–85.
64 M. Sevilla and A. B. Fuertes, *Carbon*, 2013, **56**, 155–166.
65 W. Kiciński, M. Norek and M. Bystrzejewski, *J. Phys. Chem. Solids*, 2013, **74**, 101–109.
66 Z. G. Shi, F. Chen, J. Xing and Y. Q. Feng, *J. Chromatogr. A*, 2009, **1216**, 5333–5339.
67 L. Wang, Q. Zhang, S. Chen, F. Xu, S. Chen, J. Jia, H. Tan, H. Hou and Y. Song, *Anal. Chem.*, 2014, **86**, 1414–1421.
68 Y. Song, X. Lu, Y. Li, Q. Guo, S. Chen, L. Mao, H. Hou and L. Wang, *Anal. Chem.*, 2016, **88**, 1371–1377.
69 P. A. Goodman, H. Li, Y. Gao, Y. F. Lu, J. D. Stenger-Smith and J. Redepenning, *Carbon*, 2013, **55**, 291–298.
70 C. C. Kung, P. Y. Lin, F. J. Buse, Y. Xue, X. Yu, L. Dai and C. C. Liu, *Biosens. Bioelectron.*, 2014, **52**, 1–7.
71 L. Y. Xu, Z. G. Shi and Y. Q. Feng, *Microporous Mesoporous Mater.*, 2008, **115**, 618–623.
72 G. Hasegawa, K. Kanamori and K. Nakanishi, *Microporous Mesoporous Mater.*, 2012, **155**, 265–273.
73 C. Bernal, S. Escobar, L. Wilson, A. Illanes and M. Mesa, *Carbon*, 2014, **74**, 96–103.
74 W. Sebai, S. Ahmad, N. Brun, T. Cacciaguerra, D. Cot, A. Boccheciampe, P. Chaurand, C. Levard, M. P. Belleville, J. Sanchez-Marcano and A. Galarneau, *Chem. Mater.*, 2023, **35**, 8464–8482.
75 Y. Zhang, Y. Wang, Y. Tang, R. Li and Y. Ji, *Anal. Methods*, 2019, **11**, 2465–2472.
76 L. Wang, Y. Zhao, Y. Zhang, T. Zhang, J. Kool, G. W. Somsen, Q. Wang and Z. Jiang, *J. Chromatogr. A*, 2018, **1563**, 135–143.
77 J. Ma, L. Zhang, Z. Liang, W. Zhang and Y. Zhang, *J. Sep. Sci.*, 2007, **30**, 3050–3059.
78 N. Li, W. Zheng, Y. Shen, L. Qi, Y. Li, J. Qiao, F. Wang and Y. Chen, *J. Sep. Sci.*, 2014, **37**, 3411–3417.
79 T. Hong, X. Yang, Y. Xu and Y. Ji, *Anal. Chim. Acta*, 2016, **931**, 1–24.
80 Ç. Kip, C. Demir and A. Tuncel, *J. Chromatogr. A*, 2017, **1502**, 14–23.
81 Q. C. Wang, F. Svec and J. M. J. Fréchet, *Anal. Chem.*, 1993, **65**, 2243–2248.
82 A. Kurganov, *Anal. Chim. Acta*, 2013, **775**, 25–40.
83 D. Moravcová, A. H. Rantamäki, F. Duša and S. K. Wiedmer, *Electrophoresis*, 2016, **37**, 880–912.
84 E. Candish, A. Khodabandeh, M. Gaborieau, T. Rodemann, R. A. Shellie, A. A. Gooley and E. F. Hilder, *Anal. Bioanal. Chem.*, 2017, **409**, 2189–2199.
85 E. G. Vlakh, M. A. Stepanova, Y. M. Korneeva and T. B. Tennikova, *J. Chromatogr. B: Anal. Technol. Biomed. Life Sci.*, 2016, **1029–1030**, 198–204.
86 E. Calleri, C. Temporini, F. Gasparrini, P. Simone, C. Villani, A. Ciogli and G. Massolini, *J. Chromatogr. A*, 2011, **1218**, 8937–8945.
87 D. Josic and J. G. Clifton, *J. Chromatogr. A*, 2007, **1144**, 2–13.

88 S. Jiang, Z. Zhang and L. Li, *J. Chromatogr. A*, 2015, **1412**, 75–81.
89 M. Naldi, U. Černigoj, A. Štrancar and M. Bartolini, *Talanta*, 2017, **167**, 143–157.
90 K. Meller, P. Pomastowski, M. Szumski and B. Buszewski, *J. Chromatogr. B: Anal. Technol. Biomed. Life Sci.*, 2017, **1043**, 128–137.
91 J. Křenková and F. Foret, *Electrophoresis*, 2004, **25**, 3550–3563.
92 K. W. Ro, R. Nayak and D. R. Knapp, *Electrophoresis*, 2006, **27**, 3547–3558.
93 M. Bartolini, N. H. Greig, Q. Yu and V. Andrisano, *J. Chromatogr. A*, 2009, **1216**, 2730–2738.
94 J. Sproß and A. Sinz, *Anal. Bioanal. Chem.*, 2009, **395**, 1583–1588.
95 J. Urban, F. Svec and J. M. J. Fréchet, *Biotechnol. Bioeng.*, 2012, **109**, 371–380.
96 C. Delattre, P. Michaud and M. A. Vijayalakshmi, *J. Chromatogr. B: Anal. Technol. Biomed. Life Sci.*, 2008, **861**, 203–208.
97 M. V. Volokitina, K. S. Bobrov, K. Piens, E. V. Eneyskaya, T. B. Tennikova, E. G. Vlakh and A. A. Kulminskaya, *Biotechnol. J.*, 2015, **10**, 210–221.
98 F. Coro, L. Di Pietro, S. Micalizzi, A. Bertei, G. Gallone, A. M. Raspolli Galletti, A. Ahluwalia and C. De Maria, *Chem. Eng. Sci.*, 2024, **285**, 119590.
99 J. F. A. Valente, T. S. Carreira, J. R. Dias, F. Sousa and N. Alves, *Pharmaceutics*, 2022, **14**, 2266.
100 S. Fernandez-Velayos, G. Vergara, J. M. Olmos, J. Sanchez-Marcos, N. Menendez, P. Herrasti and E. Mazarío, *Sci. Total Environ.*, 2024, **906**, 167376.
101 J. Ye, T. Chu, J. Chu, B. Gao and B. He, *ACS Sustainable Chem. Eng.*, 2019, **7**, 18048–18054.
102 J. E. Song, W. S. Song, S. Y. Yeo, H. R. Kim and S. H. Lee, *Text. Res. J.*, 2017, **87**, 1177–1191.
103 L. Yang, Y. Guo, W. Zhan, Y. Guo, Y. Wang and G. Lu, *Microporous Mesoporous Mater.*, 2014, **197**, 1–7.
104 M. Maier, C. P. Radtke, J. Hubbuch, C. M. Niemeyer and K. S. Rabe, *Angew. Chem., Int. Ed.*, 2018, **57**, 5539–5543.
105 F. Kazenwadel, E. Biegert, J. Wohlgemuth, H. Wagner and M. Franzreb, *Eng. Life Sci.*, 2016, **16**, 560–567.
106 M. S. Sarwar, U. Simon and S. Dimartino, *J. Chromatogr. A*, 2021, **1646**, 462125.
107 G. M. Whitesides and A. D. Stroock, *Phys. Today*, 2001, **54**, 42–48.
108 W. Reschetilowski, *Microreactors in Preparative Chemistry Practical Aspects in Bioprocessing, Natanotechnology, Catalysis and more*, Wiley-VCH Verlag GmbH & Co. KGaA, Weinheim, Germany, 2013.
109 F. G. Bessoth, A. J. DeMello and A. Manz, *Anal. Commun.*, 1999, **36**, 213–215.
110 A. D. Stroock, S. K. W. Dertinger, A. Ajdari, I. Mezić, H. A. Stone and G. M. Whitesides, *Science*, 2002, **295**, 647–651.
111 Z. Yang, S. Matsumoto, H. Goto, M. Matsumoto and R. Maeda, *Sens. Actuators, A*, 2001, **93**, 266–272.
112 T. Rohr, C. Yu, M. H. Davey, F. Svec and J. M. J. Fréchet, *Electrophoresis*, 2001, **22**, 3959–3967.
113 M. Heule, K. Rezwan, L. Cavalli and L. J. Gauckler, *Adv. Mater.*, 2003, **15**, 1191–1194.
114 S. Whitaker, *Ind. Eng. Chem. Res.*, 1969, **61**, 15–28.
115 J. Duan, Z. Liang, C. Yang, J. Zhang, L. Zhang, W. Zhang and Y. Zhang, *Proteomics*, 2006, **6**, 412–419.
116 V. Dore, D. Tsaoulidis and P. Angeli, *Chem. Eng. Sci.*, 2012, **80**, 334–341.
117 M. N. Kashid and D. W. Agar, *Chem. Eng. J.*, 2007, **131**, 1–13.
118 P. Garstecki, M. J. Fuerstman, H. A. Stone and G. M. Whitesides, *Lab Chip*, 2006, **6**, 437–446.
119 A. L. Dessimoz, L. Cavin, A. Renken and L. Kiwi-Minsker, *Chem. Eng. Sci.*, 2008, **63**, 4035–4044.
120 M. N. Kashid, I. Gerlach, S. Goetz, J. Franzke, J. F. Acker, F. Platte, D. W. Agar and S. Turek, *Ind. Eng. Chem. Res.*, 2005, **44**, 5003–5010.
121 N. D. M. Raimondi, L. Prat, C. Gourdon and P. Cognet, *Chem. Eng. Sci.*, 2008, **63**, 5522–5530.
122 H. Katou, R. Miyake and T. Terayama, *JSME Int. J.*, 2005, **48**, 350–355.
123 M. Riccaboni, E. La Porta, A. Martorana and R. Attanasio, *Tetrahedron*, 2010, **66**, 4032–4039.
124 D. F. Rivas, P. Cintas and H. J. G. E. Gardeniers, *Chem. Commun.*, 2012, **48**, 10935–10947.
125 J. J. John, S. Kuhn, L. Braeken and T. Van Gerven, *Chem. Eng. Process.*, 2016, **102**, 37–46.
126 P. Hajiani and F. Larachi, *Chem. Eng. J.*, 2012, **203**, 492–498.
127 M. Rahimi, O. Jafari and A. Mohammdifar, *Chem. Eng. Process.*, 2017, **111**, 79–88.
128 Y. Wang, J. Zhe, B. T. F. Chung and P. Dutta, *Microfluid. Nanofluid.*, 2008, **4**, 375–389.
129 N. Azimi, M. Rahimi and N. Abdollahi, *Chem. Eng. Process.*, 2015, **97**, 12–22.
130 E. Abraham, G. N. Mukunthan Sulochana, B. Soundarajan and S. Narayanasamy, *Ind. Eng. Chem. Res.*, 2017, **56**, 10845–10855.
131 K. Szymańska, K. Odrozek, A. Zniszczoł, W. Pudło and A. B. Jarzębski, *Chem. Eng. J.*, 2017, **315**, 18–24.
132 K. Zielińska, K. Szymańska, R. Mazurkiewicz and A. Jarzębski, *Tetrahedron: Asymmetry*, 2017, **28**, 146–152.
133 D. J. Strub, K. Szymańska, Z. Hrydziuszko, J. Bryjak and A. B. Jarzębski, *React. Chem. Eng.*, 2019, **4**, 587–594.
134 A. Liese and L. Hilterhaus, *Chem. Soc. Rev.*, 2013, **42**, 6236–6249.
135 R. C. Rodrigues, C. Ortiz, Á. Berenguer-Murcia, R. Torres and R. Fernández-Lafuente, *Chem. Soc. Rev.*, 2013, **42**, 6290–6307.
136 Y. Zhang, J. Ge and Z. Liu, *ACS Catal.*, 2015, **5**, 4503–4513.
137 C. Mateo, J. M. Palomo, G. Fernandez-Lorente, J. M. Guisan and R. Fernandez-Lafuente, *Enzyme Microb. Technol.*, 2007, **40**, 1451–1463.
138 R. A. Sheldon and S. van Pelt, *Chem. Soc. Rev.*, 2013, **42**, 6223–6235.
139 E. G. Griffin and J. M. Nelson, *J. Am. Chem. Soc.*, 1916, **38**, 1109–1115.

140 T. Tosa, T. Mori, N. Fuse and I. Chibata, *Biotechnol. Bioeng.*, 1967, **9**, 603–615.
141 A. I. Kallenberg, F. Van Rantwijk and R. A. Sheldon, *Adv. Synth. Catal.*, 2005, **347**, 905–926.
142 E. M. M. Abdelraheem, H. Busch, U. Hanefeld and F. Tonin, *React. Chem. Eng.*, 2019, **4**, 1878–1894.
143 U. Hanefeld, L. Gardossi and E. Magner, *Chem. Soc. Rev.*, 2009, **38**, 453–468.
144 R. C. Rodrigues, Á. Berenguer-Murcia, D. Carballares, R. Morellon-Sterling and R. Fernandez-Lafuente, *Biotechnol. Adv.*, 2021, **52**, 107821.
145 N. A. Mohidem, M. Mohamad, M. U. Rashid, M. N. Norizan, F. Hamzah and H. b. Mat, *J. Compos. Sci.*, 2023, **7**, 488.
146 N. R. Mohamad, N. H. C. Marzuki, N. A. Buang, F. Huyop and R. A. Wahab, *Biotechnol. Biotechnol. Equip.*, 2015, **29**, 205–220.
147 L. Van Den Biggelaar, P. Soumillion and D. P. Debecker, *Catalysts*, 2017, **7**, 54.
148 J. Coloma, Y. Guiavarc'h, P. L. Hagedoorn and U. Hanefeld, *Catal. Sci. Technol.*, 2020, **10**, 3613–3621.
149 M. P. Van Der Helm, P. Bracco, H. Busch, K. Szymańska, A. B. Jarzębski and U. Hanefeld, *Catal. Sci. Technol.*, 2019, **9**, 1189–1200.
150 D. Stradomska, J. Coloma, U. Hanefeld and K. Szymańska, *Catal. Sci. Technol.*, 2022, **12**, 3356–3362.
151 U. Hanefeld, *Chem. Soc. Rev.*, 2013, **42**, 6308–6321.
152 J. Coloma, L. Teeuwisse, M. Afendi, P. L. Hagedoorn and U. Hanefeld, *Catalysts*, 2022, **12**, 161.
153 K. Shortall, S. Arshi, S. Bendl, X. Xiao, S. Belochapkine, D. Demurtas, T. Soulimane and E. Magner, *Green Chem.*, 2023, **25**, 4553–4564.
154 M. V. Volokitina, E. G. Vlakh, G. A. Platonova, D. O. Vinokhodov and T. B. Tennikova, *J. Sep. Sci.*, 2013, **36**, 2793–2805.
155 L. Van Den Biggelaar, P. Soumillion and D. P. Debecker, *RSC Adv.*, 2019, **9**, 18538–18546.
156 D. Kowalczykiewicz, M. Przypis, L. Mestrom, A. Kumpf, D. Tischler, P. L. Hagedoorn, U. Hanefeld, A. Jarzębski and K. Szymańska, *Chem. Eng. J.*, 2022, **427**, 1–8.
157 C. Temporini, E. Perani, F. Mancini, M. Bartolini, E. Calleri, D. Lubda, G. Felix, V. Andrisano and G. Massolini, *J. Chromatogr. A*, 2006, **1120**, 121–131.
158 J. Mai, V. V. Abhyankar, M. E. Piccini, J. P. Olano, R. Willson and A. V. Hatch, *Biosens. Bioelectron.*, 2014, **54**, 435–441.
159 O. Behrmann, M. Hügle, F. Eckardt, I. Bachmann, C. Heller, M. Schramm, C. Turner, F. T. Hufert and G. Dame, *Micromachines*, 2020, **11**, 1–17.
160 M. V. Volokitina, A. V. Nikitina, T. B. Tennikova and E. G. Korzhikova-Vlakh, *Electrophoresis*, 2017, **38**, 2931–2939.
161 L. Bayne, R. V. Ulijn and P. J. Halling, *Chem. Soc. Rev.*, 2013, **42**, 9000–9010.
162 A. Basso, P. Braiuca, S. Cantone, C. Ebert, P. Linda, P. Spizzo, P. Caimi, U. Hanefeld, G. Degrassi and L. Gardossi, *Adv. Synth. Catal.*, 2007, **349**, 877–886.
163 P. De Santis, L. E. Meyer and S. Kara, *React. Chem. Eng.*, 2020, **5**, 2155–2184.
164 R. A. Sheldon, *Green Chem.*, 2023, **25**, 1704–1728.
165 P. Lozano and E. García-Verdugo, *Green Chem.*, 2023, **25**, 7041–7057.
166 P. Bracco, N. van Midden, E. Arango, G. Torrelo, V. Ferrario, L. Gardossi and U. Hanefeld, *Catalysts*, 2020, **10**, 15–19.
167 R. Onbas and O. Yesil-Celiktas, *Eng. Life Sci.*, 2019, **19**, 37–46.
168 X. Sun, Y. Xin, X. Wang and H. Uyama, *Colloid Polym. Sci.*, 2017, **295**, 1827–1833.
169 K. Szymańska, W. Pudło, J. Mrowiec-Białoń, A. Czardybon, J. Kocurek and A. B. Jarzębski, *Microporous Mesoporous Mater.*, 2013, **170**, 75–82.
170 Y. D. Ahn and J. H. Lee, *Biotechnol. Bioprocess Eng.*, 2018, **23**, 349–354.
171 A. M. Klibanov, *Nature*, 2001, **409**, 241–246.
172 K. Martinek and A. N. Semenov, *Biochim. Biophys. Acta, Enzymol.*, 1981, **658**, 90–101.
173 A. Ismail, S. Soultani and M. Ghoul, *J. Biotechnol.*, 1999, **69**, 135–143.
174 K. Szymańska, K. Odrozek, A. Zniszczoł, G. Torrelo, V. Resch, U. Hanefeld and A. B. Jarzębski, *Catal. Sci. Technol.*, 2016, **6**, 4882–4888.
175 P. He, G. Greenway and S. J. Haswell, *Process Biochem.*, 2010, **45**, 593–597.
176 Z. Yin, Y. Zhou, X. Liu, S. Zhang and B. P. Binks, *J. Colloid Interface Sci.*, 2023, **648**, 308–316.
177 B. Sandig and M. R. Buchmeiser, *ChemSusChem*, 2016, **9**, 2917–2921.
178 I. Dávila and J. Labidi, *Curr. Opin. Green Sustainable Chem.*, 2021, **28**, 100435.
179 C. J. Zimmermann, N. V. Bollar and S. G. Wettstein, *Biomass Bioenergy*, 2018, **118**, 163–171.
180 P. Lozano, *Green Chem.*, 2010, **12**, 555–556.
181 L. Zverina, M. Pinelo, J. M. Woodley and A. E. Daugaard, *J. Chem. Technol. Biotechnol.*, 2021, **96**, 2488–2495.
182 P. Lozano, E. García-Verdugo, R. Piamtongkam, N. Karbass, T. De Diego, M. I. Burguete, S. V. Luis and J. L. Iborra, *Adv. Synth. Catal.*, 2007, **349**, 1077–1084.
183 S. F. Mayer, W. Kroutil and K. Faber, *Chem. Soc. Rev.*, 2001, **30**, 332–339.
184 R. J. Conrado, J. D. Varner and M. P. DeLisa, *Curr. Opin. Biotechnol.*, 2008, **19**, 492–499.
185 Q. Ji, B. Wang, J. Tan, L. Zhu and L. Li, *Process Biochem.*, 2016, **51**, 1193–1203.
186 E. T. Hwang and S. Lee, *ACS Catal.*, 2019, **9**, 4402–4425.
187 M. Berovic and M. Vodopivec, *J. Chromatogr. B: Anal. Technol. Biomed. Life Sci.*, 2003, **795**, 105–113.
188 J. Luo, L. Ma, F. Svec, T. Tan and Y. Lv, *Biotechnol. J.*, 2019, **14**, 1–10.

189 C. Temporini, E. Calleri, K. Cabrera, G. Felix and G. Massolini, *J. Sep. Sci.*, 2009, **32**, 1120–1128.
190 T. C. Logan, D. S. Clark, T. B. Stachowiak, F. Svec and J. M. J. Fréchet, *Anal. Chem.*, 2007, **79**, 6592–6598.
191 J. Yin, T. Xu, N. Zhang and H. Wang, *Anal. Chem.*, 2016, **88**, 7730–7737.
192 J. Yin, S. Chen, N. Zhang and H. Wang, *ACS Appl. Mater. Interfaces*, 2018, **10**, 21883–21890.
193 F. Rinaldi, J. Fernández-Lucas, D. de la Fuente, C. Zheng, T. Bavaro, B. Peters, G. Massolini, F. Annunziata, P. Conti, I. de la Mata, M. Terreni and E. Calleri, *Bioresour. Technol.*, 2020, **307**, 123258.
194 E. Calleri, G. Cattaneo, M. Rabuffetti, I. Serra, T. Bavaro, G. Massolini, G. Speranza and D. Ubiali, *Adv. Synth. Catal.*, 2015, **357**, 2520–2528.
195 G. Cattaneo, M. Rabuffetti, G. Speranza, T. Kupfer, B. Peters, G. Massolini, D. Ubiali and E. Calleri, *ChemCatChem*, 2017, **9**, 4614–4620.
196 F. Hollmann, I. W. C. E. Arends and K. Buehler, *ChemCatChem*, 2010, **2**, 762–782.
197 K. Bachosz, J. Zdarta, M. Bilal, A. S. Meyer and T. Jesionowski, *Sci. Total Environ.*, 2023, **868**, 161630.
198 X. Wang, T. Saba, H. H. P. Yiu, R. F. Howe, J. A. Anderson and J. Shi, *Chem*, 2017, **2**, 621–654.
199 A. I. Benítez-Mateos, B. Nidetzky, J. M. Bolivar and F. López-Gallego, *ChemCatChem*, 2018, **10**, 654–665.
200 B. Reus, M. Damian and F. G. Mutti, *J. Flow Chem.*, 2024, **14**, 219–238.
201 Q. Chen, Y. Wang and G. Luo, *ChemSusChem*, 2022, **16**, e202201654.
202 M. Baccour, A. Lamotte, A. Lamotte, K. Sakai, E. Dubreucq, A. Mehdi, K. Kano, A. Galarneau, J. Drone and N. Brun, *Green Chem.*, 2020, **22**, 3727–3733.
203 G. Chen, Z. Wu and Y. Ma, *J. Biotechnol.*, 2015, **196–197**, 52–57.
204 Y. Li, H. Liang, L. Sun, J. Wu and Q. Yuan, *Biotechnol. Lett.*, 2013, **35**, 915–919.
205 Z. Wang, M. Etienne, F. Quilès, G. W. Kohring and A. Walcarius, *Biosens. Bioelectron.*, 2012, **32**, 111–117.
206 M. Montagné and J. L. Marty, *Anal. Chim. Acta*, 1995, **315**, 297–302.
207 M. Zhang, C. Mullens and W. Gorski, *Anal. Chem.*, 2007, **79**, 2446–2450.
208 H. Zhou, Z. Zhang, P. Yu, L. Su, T. Ohsaka and L. Mao, *Langmuir*, 2010, **26**, 6028–6032.
209 J. Britton, S. Majumdar and G. A. Weiss, *Chem. Soc. Rev.*, 2018, **47**, 5891–5918.
210 C. J. Hartley, C. C. Williams, J. A. Scoble, Q. I. Churches, A. North, N. G. French, T. Nebl, G. Coia, A. C. Warden, G. Simpson, A. R. Frazer, C. N. Jensen, N. J. Turner and C. Scott, *Nat. Catal.*, 2019, **2**, 1006–1015.